

# Developing Compatible Techniques for Magnetic Resonance Imaging of Stroke Pathophysiology

By

Mathew E Brevard

A Thesis

Submitted to the Faculty

of the

WORCESTER POLYTECHNIC INSTITUTE

in partial fulfillment of the requirements for the

Degree of Master of Science

in

Biology

by

---

December, 2002

APPROVED:

---

Dr. Craig F. Ferris, Advisor

---

Dr. Elizabeth F. Ryder, Advisor

---

Dr. Daniel G. Gibson III, Advisor

# Abstract

Stroke is the most prevalent neurological disease facing our nation today. Treatments, however, are few and insufficient at reducing the impact of this neurological condition. Experimental animal models are important to improving our understanding of stroke, and for developing new therapies to counter the pathology of stroke. Magnetic Resonance Imaging is the leading tool for the non invasive investigation of stroke pathophysiology. While most MRI work in animals is conducted under anesthesia, anesthesia has profound effects on cerebral circulation and metabolism, and can affect stroke outcome.

Several novel methods were combined with MRI compatible physiologic monitoring equipment to conduct stroke studies in conscious animals. Stress was studied as a factor in these studies and conditioning was utilized to reduce the impact of stress on the animals physiology. Models of both occlusive and hemorrhagic strokes were successfully implemented within the MRI apparatus. Lastly, experiments using a macrosphere model showed evidence of a pathophysiologic difference between awake and anesthetized animals that undergo stroke.

## **Acknowledgements**

I would like to sincerely thank the following individuals for their contribution to my knowledge of science and philosophy.

Craig F. Ferris, Ph.D.

Jean A. King, Ph.D.

Department of Psychiatry, University of Massachusetts Medical School

Liz Ryder, Ph.D.

Dan Gibson Ph. D.

Department of Biology, Worcester Polytechnic Institute

Tibo Gerriets M.D.

Justus-Liebig-Universität. Giessen, Germany

Mark Fisher M.D.

Fuhai Li M.D.

UmassMemorial Dept. of Neurology

John R. Ives Bc.S.

Harvard School of Medicine Dept of Neurology

Robert M. K. W. Lee, Ph.D

Department of Anesthesia, McMaster University, Hamilton, Ontario

I would also like to thank Tara Messenger for her assistance with my work.

# Table of Contents

<b>Abstract</b>	<b>ii</b>
<b>Acknowledgements</b>	<b>iii</b>
<b>List of Figures</b>	<b>vi</b>
<b>List of Tables</b>	<b>vi</b>

---

## **1. INTRODUCTION**

---

## **2. BACKGROUND**

---

<b>2.1</b>	<b>STROKE</b>	<b>4</b>
<b>2.2</b>	<b>STROKE PATHOPHYSIOLOGY</b>	<b>5</b>
<b>2.3</b>	<b>MRI AND EEG</b>	<b>8</b>
<b>2.4</b>	<b>STRESS</b>	<b>9</b>
<b>2.5</b>	<b>ANESTHESIA</b>	<b>10</b>
<b>2.6</b>	<b>NEUROPROTECTION</b>	<b>11</b>
<b>2.7</b>	<b>MODELS</b>	<b>12</b>
<b>2.8</b>	<b>HEMORRHAGIC STROKE MODELS</b>	<b>14</b>
2.8.1	SUBARACHNOID HEMORRHAGE (SAH) MODELS	14
2.8.2	SPONTANEOUS HEMORRHAGIC MODEL	17
2.8.3	ICH MODELS	17
<b>2.9</b>	<b>OCCLUSIVE STROKE MODELS</b>	<b>18</b>
2.9.1	SUTURE MIDDLE CEREBRAL ARTERY OCCLUSION (MCAO) MODEL	19
2.9.2	MACROSPHERE MODEL	20
2.9.3	PHOTOTHROMBOSIS MODEL	21
<b>2.10</b>	<b>HISTOLOGY</b>	<b>21</b>
<b>2.11</b>	<b>CONCLUSION</b>	<b>23</b>

---

## **3. METHODS**

---

<b>3.1</b>	<b>HEART RATE (HR)</b>	ERROR! BOOKMARK NOT DEFINED.
<b>3.2</b>	<b>FEMORAL ARTERY CATHETERIZATION</b>	ERROR! BOOKMARK NOT DEFINED.
<b>3.3</b>	<b>CEREBROSPINAL FLUID PRESSURE (CSFP) MEASUREMENT</b>	<b>25</b>
<b>3.4</b>	<b>ELECTROENCEPHALOGRAPHY (EEG)</b>	<b>25</b>
<b>3.5</b>	<b>ANESTHESIA METHODS</b>	<b>26</b>
<b>3.6</b>	<b>PILOT STRESS STUDIES METHODS</b>	<b>27</b>
<b>3.7</b>	<b>HISTOLOGY METHODS</b>	<b>27</b>
<b>3.8</b>	<b>MODEL METHODS</b>	<b>31</b>
3.8.1	SUTURE SAH	31
3.8.2	SPSHR MODEL	32
3.8.3	ICH MODEL	33

3.8.4	MACROSPHERE MODEL		34
3.8.5	SUTURE MCAO METHOD	<b>ERROR! BOOKMARK NOT DEFINED.</b>	
		<b>36</b>	
3.8.6	PHOTOTHROMBOSIS METHOD		36
3.8.7	NEUROLOGIC SCORING		37
3.9	STATISTICS		37
<b>4. RESULTS</b>			<b>38</b>
4.1	PHYSIOLOGY SYSTEM		38
4.2	ANESTHESIA		47
4.3	PILOT STRESS STUDY		48
4.4	MODELS		50
4.4.1	SPSHR MODEL		51
4.4.2	SAH MODEL		53
4.4.3	ICH MODEL		55
4.4.4	PHOTOTHROMBOSIS MODEL:		58
4.4.5	MACROSPHERE AND SUTURE MCAO MODEL		59
<b>5. DISCUSSION</b>			<b>69</b>
5.1	PHYSIOLOGY SYSTEM		69
5.2	ANESTHESIA		70
5.3	STRESS STUDIES		71
5.4	STROKE MODELS		71
5.6	HISTOLOGY		75
5.6	MRI AS A TOOL TO INVESTIGATE STROKE		76
<b>6. REFERENCES</b>			<b>80</b>
<b>7. LIST OF ABBREVIATIONS</b>			<b>86</b>

## List of figures

**Figure 1:** Latex impregnated cerebral arteries of the base of the brain.

**Figure 2:** Diagram of the catheter designed for inducing SAH in the bore of the magnet.

**Figure 3:** A sample physiologic trace for an animal in the MRI restrainer using only non invasive sensors.

**Figure 4:** Entering the room during BP monitoring affects the tail perfusion in rats.

**Figure 5:** Direct blood pressure, respiration rate, and intracranial pressure waveforms.

**Figure 6:** A sample EEG trace in an animal waking from anesthesia.

**Figure 7:** Effects of atipamazole on a medetomidine anesthetized rat.

**Figure 8:** Acclimation of animals (n=6) to restraint stress over the course of daily restraint.

**Figure 9:** Physiologic parameters on a SPSHR model of induced hemorrhage and control animal.

**Figure 10:** Physiology trace of a SAH in an anesthetized rat.

**Figure 11:** Postmortem condition of the brain after SAH induction.

**Figure 12:** Brain and slices of ICH induction.

**Figure 13:** Physiologic parameters of sedated and awake preparations of ICH.

**Figure 14:** Brain of an animal after photothrombotic stroke formation.

**Figure 15:** Location of macrospheres in the cerebral arteries of the sedated group.

**Figure 16:** Location of macrospheres in the cerebral arteries of the awake group.

**Figure 17:** Suture MCAO brain showing the suture lodged into the anterior cerebral artery.

**Figure 18:** Histology of ischemic lesions.

**Figure 19:** Physiologic profile of a macrosphere and suture MCAO Model in an anesthetized, awake, and awake control animal.

## List of Tables

**Table 1:** The models that were developed for, or used in this study.

**Table 2:** The success rate of macrosphere induced stroke in study subjects.

**Table 3:** Location of spheres in the cerebral arteries.

**Table 4:** Blood gas and metabolite concentrations in animals pre and post stroke.

**Table 5:** Outcome of the macrosphere stroke subjects 24 hours after stroke.

**Table 6:** Physiologic measures of the awake, anesthetized, and suture MCAO groups.

# 1. Introduction

**S**troke constitutes a major threat to the health of Americans. It is the 3<sup>rd</sup> leading killer, causing death in 20% of the 700,000 Americans that suffer a stroke each year. It is also the predominant cause of disabilities that require hospitalization, with stroke patients exacting 30-40 billion dollars per year in related costs. Stroke occurs in two major forms where the cerebral arteries either rupture (hemorrhagic) or become blocked (occlusive).

There is no standard surgical or pharmacological intervention for the treatment of stroke, but early and accurate diagnosis is crucial to improving the outcome for the patient. The most effective medication for stroke is only indicated for use with 4% of stroke victims. Careful monitoring and manipulation of the patient's physiology is used to treat the remaining majority of strokes. Variables such as intracranial pressure and systemic blood pressures are controlled to provide the patient with the optimum recovery scenario. Most of the current practices have evolved from clinical results, rather than experimentation.

Clinical diagnosis relies on accurate imaging technologies that are sensitive to the multitude of stroke pathologies. The location and mechanism of stroke must be known before treatment of any kind can be initiated (Tintinall, 2000). This is of vital importance, since treatments for one type of stroke can be harmful to patients suffering from the other form.

Magnetic Resonance Imaging (MRI) is one tool that is providing for more accurate assessment of stroke in the clinic. It is also a valuable research tool for understanding stroke pathology. MRI provides a noninvasive tool to study the morphological changes that occur to the brain following cerebrovascular insult. MRI has also recently been developed as a tool to track changes in cerebral blood flow and metabolism. The capacity for MRI to work in these two modalities makes it a powerful tool to study the complete mechanism of stroke.

Of equal importance for stroke research are accurate animal models of stroke. Models exist for each type of stroke to help researchers understand the physiologic and pathologic changes that accompany stroke. Models also provide a testing ground for interventions and therapies. These models usually involve an invasive mechanism to block or rupture the cerebral arteries, and the strokes have always been initiated in anesthetized animals.

Anesthesia plays an important role in current stroke studies. Most models require surgical preparation under anesthesia and MRI studies require that animals remain motionless for imaging sessions. This immobilization is usually accomplished with constant anesthesia. Since anesthesia has such a profound effect on cerebral circulation and metabolism, many researchers (Warner, 1995; Jacewicz, 1986; Molinari, 1986) argue that the design of the experiment, in regard to what anesthetics are used and how they are administered, has a major effect on the conclusion of the stroke study.

To avoid this caveat, our goal was to adapt stroke models to use awake animals. A stroke model where the animal is awake is more complicated to

prepare and experiment on than one where the animal is anesthetized. Also, working with the model while the animal is located in the bore of the MRI magnet adds spatial problems that do not arise when the animal is anesthetized and freely accessible on the bench top. Typical monitoring equipment for the animal is often incompatible with the MRI machine, so new equipment and methods for compatibility with the space and electromagnetic limitations of the MRI environment had to be developed. Despite these issues, the benefit of inducing a stroke while the animal is within the MRI has several experimental advantages; providing more realistic data because the animal is awake, allowing each animal to serve as its own control by collecting data before the stroke occurs, and utilizing the non invasive techniques or MRI to study stroke pathophysiology while it occurs.

## 2. Background

### 2.1 *Stroke*

**S**troke occurs in two major forms. Ischemic stroke results from a blockage of blood flow to parts of the brain, while hemorrhagic stroke occurs when blood passes the blood brain barrier (BBB) through a breach in the arteries. In some cases both forms of stroke occur simultaneously, or when one converts to the other. Both mechanisms disrupt the normal delivery of nutrients and removal of byproducts to and from cells and can quickly cause damage. This starvation/toxic damage can begin within 30 seconds and can become irreversible within 6 minutes.

Ischemic strokes are the most common form of cerebrovascular disease and comprise 80-85% of cases. Thrombosis, or gradual build up of fibrous deposits along the arterial lining, is the primary cause of ischemic stoppage of blood flow. Thrombosis is primarily caused by atherosclerotic disease. Embolism, the lodging of a free floating particle, accounts for one quarter of ischemic strokes. Hypoperfusion is a much rarer cause of ischemia, wherein blood flow is lowered on a hemispheric scale.

The remaining 20% of strokes occur via hemorrhage. Hemorrhagic strokes unfortunately carry with them a bleak prognosis. The 30-day survival rate is 30-50%. Intracerebral hemorrhage (ICH) is the major mechanism in this category and is characterized by bleeding within the parenchymal space.

Subarachnoid hemorrhages (SAH) are half as common as ICH and form when extra parenchymal bleeding occurs. After a SAH occurs, the major causes of mortality are re-bleeding and vasospasm.

## **2.2 Stroke Pathophysiology**

The brain has the most consistent blood flow of any organ in the body. It constantly uses 20% of all oxygen consumed and it maintains perfusion at steady levels despite any peripheral changes. Perfusion through the cerebrovascular system is determined by the mean arterial blood pressure (MABP), intracranial pressure (ICP), venous pressure (which is equal to the ICP), cerebral perfusion pressure (CPP), and cerebral blood flow (CBF). The MABP is regulated by the primary extracranial arteries to keep an even CPP throughout the brain, and in fact the CPP is determined by the equation:  $CPP = MABP - ICP$ . The CPP in turn affects the CBF. These factors are very important during stroke as they can determine how the stroke progresses.

In order to keep perfusion constant through the brain, the carotid and vertebral arteries are responsible for a large amount of the regulation of pressure in the brain (Heistad, 1983). In cases of hypertension, the cerebral microvascular pressures are not as elevated as systemic pressures. Autoregulation is responsible for maintaining CBF despite systemic changes in MABP. An animal with hypertension is able to regulate blood flow at much higher pressures than normotensive animals which allows CBF to be maintained. When pressures are sufficiently high, autoregulation can not compensate for changes in pressure and CBF and CPP will increase linearly with MABP.

When blood flow to the brain is disrupted, changes begin immediately. Glucose supplies are quickly diminished, neuronal function is lost within seconds, and hypoxia begins to set in as oxygen is used up within minutes. Byproducts accumulate and begin to damage the already compromised cells and within 6 minutes permanent ischemic damage can set in (Jacewicz, 1986). These changes that occur metabolically and physiologically within the first few minutes of trauma are extremely important to the outcome of the stroke (Nath, 1987).

As the vascular and metabolic changes occur, the brain tries to compensate. The excess metabolites, primarily CO<sub>2</sub>, have an instant effect on the surrounding vasculature, and perfusion is increased via collateral flow. In a large lesion, there exists an ischemic core that is void of any blood supply and becomes necrotic. This core grows within the watershed of the affected arteries over the first few hours. The surrounding “penumbra”, the viable tissue that surrounds a necrotic lesion, relies on the redundancy of the cerebral vasculature to remain perfused.

After 2 hours the ischemic lesion is mostly defined; however, edema is still progressing. The major cause of edema is the build up of cytotoxins that alter the exchange of intra and extra cellular water. After edema, there is a prolonged period of neuronal loss and ischemic damage progression that extends for weeks (Kawaguchi, 2000).

The sequale following hemorrhagic stroke are dependent on how the bleeding occurs. During an extraparenchymal bleed, such as an SAH, the ruptured vessel is usually a major artery; thus, a large amount of blood enters the

intracranial cavity at a high pressure. This causes an acute increase in ICP and a decrease in CBF and CPP. This reduced blood flow can be sustained for several minutes during which time ischemic damage can set in. Blood does not cross the BBB, however, so the cellular changes are attributed more to reduced blood flow. The incidence and progression of stroke is affected by hypertension. Studies have noted that the incidence of hemorrhage is linked to chronic hypertension (Coutard, 2000) while the severity is linked to the maximal blood pressure and acute hypertension (Benveniste, 2000).

During an ICH the blood comes directly into contact with the cells of the brain. The tissue contains the bleeding, so ICP, CBF, and CPP are not as drastically altered as in an SAH. A slight increase in ICP is accompanied by a drop in CPP and CBF after an ICH, but these may not be extreme enough to cause ischemia (Patel, 1999). Cytotoxins and other compounds from the blood can damage the cells that are within the bleeding zone, however.

In the longterm case, both forms of hemorrhage alter the cerebral vasculature in devastating ways. Vasospasm is a reaction to hemorrhage wherein the vessels all contract to the point that blood flow is severely suppressed. Vasospasm is the primary cause of ischemia in hemorrhagic strokes, but it usually takes several hours or more to set in.

One stroke mechanism can accompany or convert to another. As mentioned above, ischemia usually accompanies hemorrhagic strokes. Also, occlusive strokes can hemorrhage. An occlusion in the arteries prompts the thrombolytic compounds to attack the blockage. This can cause a weakening in

the arterial wall and eventually rupture. Metabolites can also weaken arteries, and if blood flow and pressure is reestablished after a period of ischemia, hemorrhage can occur.

The ICP and MABP determine the cerebral circulation during stroke, but important questions about clinical manipulations of these factors remain untested in experimental models. For instance, how does the body react to a hemorrhage, and is it detrimental or therapeutic for us to increase or decrease ICP or MABP during the recovery period? If a clinician lowers the CPP to reduce bleeding, then ischemia could be induced; however, increasing CPP to keep tissue supplied with blood could cause further hemorrhage. The ability to study peripheral and cerebral physiology and the subsequent outcome in an accurate model of stroke is critically important to medicine.

### **2.3 MRI and EEG**

Clinically, imaging is essential to the treatment of stroke. Computed Tomography (CT) is a readily available technology for imaging the brain; however, it is unable to detect stroke until 12 hours after the incident. Conventional MRI sequences are able to detect stroke after 3 hours, and newer sequences can detect stroke as early as 4 minutes after they occur. Still newer sequences hold the promise of being able to detect the penumbra, or the viable region that surrounds a stroke lesion. (Tintinall, 2000)

Electroencephalography (EEG) can be used to assess the consciousness of the subject while undergoing stroke and the viability of regions of the brain after ischemia. EEG provides a measure of the intensity and synchronicity of

neuronal activity in the area of the electrode. In a conscious brain, the neurons are firing quickly and at different times. The resulting signals have relatively low amplitudes and high frequencies and are called Beta and Alpha Waves. Beta waves are present with an active brain and have the lowest amplitude and highest frequency (14 Hz and above). Alpha waves are present in times of conscious restfulness (8-13 Hz). When a brain is in an increasingly restful state, less activity is present in the neurons. The activity that is present is generally more synchronized and slower. These synchronized electrical events are additive and the resulting wave from a group of neurons has a higher amplitude. The Theta and delta waves that are associated with unconsciousness are high in amplitude and low in frequency (4-7 Hz for theta and less than 4 Hz for delta).

Measuring EEG in the dynamic, electromagnetic environment of the MRI magnet poses a unique problem. Aside from the fact that these two modalities interfere with each other when information is being acquired, the hardware for each can cause interference with the other (Ives, 1993).

## **2.4 Stress**

Conscious restraint can be a major form of stress for animals in awake models. Aside from affecting the general well being of the animal, stress can alter the physiology of an animal, and possibly affect the outcome of the stroke. While it is possible to limit stress by using certain drugs, these have many of the same complications that anesthetics do when considering stroke outcome. It is important to determine what component stress might have in awake models by measuring physiologic and biochemical markers for stress over a period of time.

## **2.5 Anesthesia**

Anesthesia can have powerful effects on the pathophysiology of stroke. These effects are attributed to the ability of anesthesia to alter cerebral circulation and provide neuroprotection. Anesthesia also has a strong effect on imaging techniques that are sensitive to changes in cerebral circulation. A depression in BOLD (Blood Oxygen Level Dependent) based signal in anesthetized animals has been demonstrated (Lahti, 1998). Anesthesia can affect the physiology of an animal model in ways that can alter the outcome of stroke, such as lowering of body temperature, or inducing hypercarbia (Jacewicz, 1986). Many studies have also shown neuroprotective effects of anesthesia (Kawaguchi, 2000; Warner 1991, 1995; Nellgard, 2000).

Most studies on the effects of anesthesia on stroke outcome must base their conclusions on a comparison between two anesthetics. Even “awake” stroke studies use animals that are under the effects of anesthesia for at least the first 8 minutes of their stroke (Warner, 1995). This period is of significant importance since ischemic damage can occur during this time (Nellgard, 2000).

All forms of anesthesia work by inhibiting neuronal activity.  $\alpha$ -Chloralose is an anesthetic agent that has minimal effects on neuronal activity and was chosen by Nakao et al (2001) to study regional blood flow and metabolism. Even this mild anesthesia reduced blood flow and metabolism in cortical areas while other structures retained function. Functional studies would be hindered by this selective suppression of certain structures while others are left functional.

The alteration of respiratory physiology and blood chemistry that accompanies inhaled anesthesia, which is the primary form of anesthesia used in MRI studies, poses unique complications to the studies. In a study that utilized an awake control animal (Warner, 1996), the animal was allowed to recover from anesthesia after surgery and was then placed in a chamber containing 40/60 O<sub>2</sub>/N<sub>2</sub>. This is consistent with the anesthetized groups who were receiving the same gas mixture via a ventilator, but it does not guarantee equivalent blood gas concentrations. It also doesn't adjust for the difference in blood pressure, metabolism and circulating catecholamines in the awake group.

## **2.6 Neuroprotection**

Neuroprotective effects of many different substances have long been noted and studied as possible therapeutic interventions for stroke victims. Anesthetics are one class of drugs that seem to offer strong neuroprotective effects. Conflicting and confusing results plague the field, and it has been remarked that every detail of the experimental setup seems to have an effect on the outcome (Jacewicz, 1986; and Warner, 1995). There is even confusion in how the neuroprotection is classified. Stroke severity can be gauged by neurological function, gross pathology, cellular morphology, or any combination of the three. While an anesthetic might offer an improved outcome along one variable, it might not show an improvement elsewhere. For instance, barbiturates produced a lower infarct volume after 96 hours when compared to isoflurane; however, there was no significant difference in neurological scoring (Warner,

1991). The progression of neuroprotection is as complex as the outcomes (Kawaguchi, 2000).

Several mechanisms have been proposed for the neuroprotective effects of anesthesia. Among the possibilities are altered cerebral blood flow, reduction of cerebral metabolism to offset the diminished supply, reduction in catecholamine levels in the brain, alteration of thermoregulation, protection from neurotoxicity of neurotransmitters, and alteration of calcium channel activity. None of these mechanisms seem to stand out as “the” source of neuroprotection. The evidence leads one to conclude that neuroprotection arises from a combination of factors.

Anesthesia also affects the actions of neuroactive compounds. For instance, anesthetics can reduce the neurotoxicity that is associated with glutamate and aspartate. Currently, studies are confounded when brain biochemistry is studied in anesthetized animals with altered neural activity and metabolism. Awake models are needed to clarify the relationship between non-anesthetic neuroprotective agents, such as calcium blockers and excitatory amino acid antagonists, and anesthesia.

## **2.7 Models**

Animal models of stroke have been developed and used for several decades. Clinical research fields, such as radiology, have benefited greatly from these models when developing new diagnostic procedures. Other fields though, such as pharmacology, have had very limited success developing new treatment strategies using the current models (Wiebers, 1990).

With all of the complications involved with anesthesia in stroke models it would be prudent to limit the presence of anesthesia on the stroke models. Ridenour et al (1992) remarked that less invasive models would allow for studies to be done in awake animals. Warner et al (1995) established an awake protocol to use as a control for studies on the effects of anesthesia on stroke pathology. Their awake model was the removal of the animal from anesthesia as quickly as possible after the occlusion of the middle cerebral artery (MCAO). They reported a typical interval of 5-8 minutes between a suture MCAO induction (when the animal was still anesthetized) and the return of the righting reflex after the anesthesia was halted. This is a very important period in stroke pathophysiology, however, and one wonders what effects the anesthesia has during this initial time.

Studying the physiologic condition of an animal, both peripheral and cerebral, is more realistic in awake models (Lahti, 1998; Demura, 1993; Molinari, 1986), since the human condition during the strokes that are being modeled does not usually involve sedation. Evidence has also shown a protective effect from anesthetic agents, and would support the elimination of anesthetics from a protocol when possible.

Several of the current stroke models of both occlusive and hemorrhagic stroke seemed adaptable to use in a conscious animal. Three occlusive models were investigated, but only one seemed feasible in awake rats. One hemorrhagic model was developed in a previous study (Brevard, 1999) and was looked at

further and two additional models were investigated for use in conscious animals.

Table 1 outlines the 6 stroke models that were looked at.

Model	SPSHR	ICH	Suture SAH	Macrosphere	Suture MCAO	Photothrombosis
Stroke Type	Intracerebral hemorrhage	Intracerebral hemorrhage	Subarachnoid hemorrhage	Permanent MCA occlusion	Permanent MCA occlusion	Small arterial occlusion
Mechanism	Spontaneous Hemorrhage	Intracerebral blood infusion	Mechanical SA artery rupture	Injected Embolism	Intraluminal occlusion	Photochemical clot formation
Conducted in awake cohorts?	Yes	Yes	Yes	Yes	No	No

Table 1: The models that were developed for, or used in this study.

## 2.8 Hemorrhagic Stroke Models

While intracranial hemorrhage occurs less often than occlusive stroke, the bleak prognosis it offers and the lack of treatment options makes hemorrhagic stroke clinically very important. Intracranial hemorrhage occurs in 2 major forms, defined by where the bleeding occurs. Intracerebral hemorrhage (ICH) occurs within the parenchyma where the bleeding is often contained, and subarachnoid hemorrhage (SAH) is bleeding into the extra parenchymal space.

Both of these forms of stroke are indicated by rapid changes in intracranial physiology, and by slower developing changes in histopathology. As in other parts of the body, CBF is regulated primarily by metabolic and neurotransmitter factors proximally, and more by pH of the surrounding tissue deeper in the brain (Patel, 1999).

### 2.8.1 Subarachnoid Hemorrhage (SAH) Models

A SAH has more global effects on the brain since the bleeding that occurs is outside of the parenchyma and is distributed quickly throughout the area of

bleeding. Aside from the immediate problems that occur during a SAH bleed, another major cause of patient decline is the onset of vasospasm. This reactive constriction of cerebral blood vessels causes a delayed and marked ischemia.

Two primary methods exist for modeling SAH. One method, the intracisternal infusion, uses the injection of unclotted blood drawn from a peripheral site, directly into the subarachnoid space via an accessible area such as the cisterna magna. Another method, the suture SAH, involves the mechanical perforation of vessels in the base of the brain. The former method is not very analogous to human SAH in the way that bleeding occurs (Schwartz, 2000) and it fails to account for the initial damage of the vessel and the effects of the autoregulatory system on the bleeding. The latter, while it is more realistic, can have very drastic effects on the neurologic condition of the animals. Since SAH is an extreme form of stroke this exaggerated model is still realistic in its pathology.

Intracisternal infusion is a popular model for SAH. Studies with an infusion of autologous blood (Brinker, 1992) show that as blood enters the parenchymal space the ICP undergoes a sharp rise. This increase does not plateau as the ICP does during a saline infusion, during a suture SAH, and during the few documented clinical SAH's in human subjects. While this ICP increase corresponds to a decrease in regional CBF (rCBF) this model does not demonstrate a realistic model of the clinical SAH. Physiologically, this model is not as appropriate as the suture model (Schwartz, 2000), and was not considered any further.

The suture model, developed by Veelken et al (1995), uses a stiff nylon suture inserted into the common carotid artery (CCA) and advanced through the internal carotid artery (ICA) to perforate the cerebral arteries. This method is easy to carry out and yields a consistent subarachnoid bleed.

Schwartz et al (2000) found a difference in intensity of hemorrhage between induction with a 3-0 and with a 4-0 suture. They found that the smaller suture created a less severe hemorrhage and had a higher survival rate in the animals. The suture SAH model can be complicated by presence of the suture within the ICA blocking blood flow, which might cause further ischemia. In this study, the authors realized that collateral flow in the rat is sufficient to overcome the permanent occlusion of the CCA that is necessary to insert the suture. This has also been noted in the suture occlusion models (Dr Li, Personal comment).

Ischemia is believed to be the important clinical contributor to brain damage in SAH. Models have shown a decrease in CBF is caused initially from reduction in CPP. But later this decrease is attributed to other factors such as vasospasm. (Bederson, 1995) Using Laser Doppler flow (LDF) it was found that as CPP began to increase, blood flow did not return to normal levels. So while perfusion pressure was adequate to supply blood to the brain, other factors were retarding its flow. This decreased flow might be attributable to reduced metabolism, however, and might not be causing ischemia. Concurrent monitoring of cerebral metabolism, blood flow, and neuronal viability could provide a more accurate explanation of what factors contribute to the damage during an SAH.

### **2.8.2 Spontaneous Hemorrhagic Model**

Spontaneous hemorrhage is often the result of a hypertensive development in an animal, which makes this type of model congruent with human stroke. This hypertension can be hereditary or iatrogenic in nature and is usually chronic. Several models of spontaneous hemorrhage exist and are amenable to study and most use animal strain based genetic factors that contribute to the prevalence of stroke. The SPSHR is one such hereditary model where each rat develops under extreme hypertension, leading to weak arteries from arteriosclerosis. The SPSHR model of spontaneous hemorrhagic stroke was developed in a previous body of work (Brevard, 1999) but required further refinement.

Hypertension can also be caused by manipulations made by investigators. Coutard et al (2000) created a fairly consistent model of cross bred rats with a unilateral nephrectomy at 12 weeks of age and conditioning with weekly doses of deoxycorticosterone and drinking water containing 1% saline. These cross-bred animals hemorrhaged 80% of the time after treatment.

### **2.8.3 ICH Models**

ICH is characterized by bleeding that occurs at the more distant cerebral arteries where the blood comes in direct contact with the neuronal tissue. Smaller changes occur in ICP, and veno-motor tone can change sufficiently as to cause vasospasm. To model this pathology, autologous blood is injected directly into a catheter that passes into the brain tissue (Nath, 1987).

Delayed ischemia after hemorrhage is attributed to altered CBF via vasospasm, altered CMR, or blood-brain barrier disruption. Patel et al (1999) noted this delayed effect in an ICH model by studying CBF 4 hours after 100  $\mu$ l autologous blood injection and found that the only region of the ICH falling below ischemic thresholds for CBF was the clot itself. They did not find significant ischemia with conventional histological staining 24 hours post stroke.

The CBF drops for about 10 minutes following ICH induction but returns to normal or near normal levels some time within 3 hours (Nath, 1987; Patel, 1999). However, this CBF drop may not be sufficient to induce any major ischemic damage. While cerebrovascular changes can resolve themselves over time (within 3 hours), permanent pathological changes are sustained during an ICH. Patel et al found pathologic damage was confined to the immediate area around the clot. They also found regional decrease in potassium that could result from cells shunting potassium in order to control cell swelling. These changes might indicate more specific cellular damage that is not detected as an ischemic lesion.

As with SAH models, temporally consistent methods for monitoring blood flow, metabolism, neuronal viability, and other factors that MRI can monitor might help researchers characterize the progress of an ICH.

## **2.9 Occlusive Stroke Models**

The primary distinction between different occlusive stroke models is whether the blockage is reversible or permanent. Both types cause ischemia, but the outcome of a reversible stroke is dependant on when and how flow is

restored. In this work, however, only permanent occlusive strokes were looked at.

### **2.9.1 Suture Middle Cerebral Artery Occlusion (MCAO) Model**

The suture method of middle cerebral artery occlusion was devised by Koizumi et al (1986) as a way to avoid craniotomy for MCAO. Known as intraluminal suture occlusion, it was revised by Longa et al (1989). Currently it is the most widely used stroke model, and has been heavily utilized for the development of new MRI sequences for stroke diagnosis. In these applications the animal is permanently anesthetized during the often very long imaging session.

Infarct size in this and other models is variable in different rat strains because of collateral flow and differences in the structure of the cerebral blood vessel (Jacewicz, 1986). Despite the variability, this method produces fairly consistent lesions to the MCA territory. Aside from obvious lesions and neurologic deficits, EEG recordings show a decrease in amplitude after MCAO (Longa, 1989).

Suture MCAO often has the long term complication of inducing hyperthermia, which is the second most important factor in ischemic lesion development after blood flow (Jacewicz, 1986). This is the result of ischemic damage in the hypothalamus resulting from blockage of the hypothalamic arteries. Warner et al state that hyperthermia is often associated with the suture MCAO model and that small changes in brain temperature can have a large

effect on the outcome. The progress of ischemic damage as it is accentuated by hyperthermia has not been studied yet.

### **2.9.2 Macrosphere Model**

The macrosphere model is a newly developed model of permanent artery occlusion in rodents (Gerriets; *Stroke*, submitted). The outcome in both neurologic scoring and lesion volume is nearly identical to the well established suture MCAO method. Briefly, permanent MCAO is induced by intraarterial embolization using six TiO<sub>2</sub> microspheres. These spheres are injected into the ICA via the neck and travel into the brain lodging in the ACA, MCA, PCA, distal ICA, (See figure J) or any combination thereof.

Other researchers have used artificial injected emboli in awake animals in the past in order to limit complications from anesthesia (Demura, 1993). The microsphere model uses the injection of thousands of microscopic spheres (50µm) into a free moving rat via an ICA catheter. Conscious animals in this model have a higher mortality rate, which is attributed to more drastic edema. This model does not correlate to any clinically prevalent stroke pathologies, however, and is of little research value.

This method produces consistent lesions without inducing hyperthermia (Gerriets et al). Suture MCAO induces hyperthermia when the suture blocks the hypothalamic arteries and causes a lesion in the hypothalamus. The macrosphere model avoids this complication since the spheres seat in the cerebral arteries well distal to the ICA bifurcation where the hypothalamic arteries seat. Another important feature of this method is the fact that the embolus

injection can be conducted remotely in an awake animal. One drawback is that this method is not reversible, unlike the suture method, and can only model permanent MCAO strokes.

### **2.9.3 Photothrombosis model**

The photothrombosis model, developed by Watson et al (1985), utilizes an oxidation from a photo-active dye injected into the vasculature. A clot is formed when this reaction is induced by energy from a light source. Endothelial cells are oxidized and platelets aggregate to form clots that embolize vessels. These clots form in any blood vessel within the range of the light and are permanent. In order to embolize a major branch of the MCA and therefore mimic human stroke, the MCA must first be located. This is not usually possible without a craniotomy, and extensive surgery is required to reach the base of the brain where the main MCA branches lie (B Watson, personal comment).

## **2.10 Histology**

Histology is the standard tool used to define the overall pathology of the stroke. It is powerful in its ability to discern the changes that occur with stroke on a macroscopic, microscopic, and biochemical level. Lesion volume is assessed based on the gross cell death within the damaged brain. More accurate indicators of cellular damage include stains for cell components and immunological stains for biochemical activity.

Kawaguchi et al (2000) pointed out the importance of delineating between two forms of ischemic damage. One, infarction, involves the necrosis of all cells, glial and neuronal. The other occurs in areas of lesser ischemia and is termed specific neuronal necrosis (SNN) and takes much longer to progress. This distinction might be important when one looks at the incongruities between stroke outcome, functional deficits, and lesion volumes as they pertain to the different types of damage occurring during stroke.

A standard dye for staining infarct volume is the hematoxylin and eosin stain. When neurons are damaged they have a high affinity to acidic dyes like eosin and “display a pyknotic nucleus.” (Sankar et al, 1997). These neurons also lose their affinity to hematoxylin, and damaged areas then show up as light pink.

Other stains for lesion volume are the tetrazolium salt based stains. These stains have an affinity for mitochondrial activity and stain viable areas. The ischemic areas are indicated by regions with a lack of stain and correlate well with MRI sequences sensitive to decreased intra and extra cellular diffusion. The drawback for tetrazolium staining is that it must be done in thick slices (1-2mm) of fresh tissue and this tissue can not be used for any other stain. Tetrazolium staining limits the user to a gross measure of ischemic volume that is also achievable non-invasively via MRI, while it excludes more sensitive microscopic examination.

Cellular integrity can be examined using stains for cellular structures. The H and E stain is used to stain for nuclei integrity. Nissl stains bind to nucleic acids

and stain nuclei and other cellular structures. The thionin stain is one such nissl stain.

## **2.11 Conclusion**

The goal of this study was to develop awake stroke models where the stroke could be induced while the animal is in an MRI machine. Such models could show investigators the changes that occur during the stroke, and the initial condition of the animal before the stroke. These goals had not been widely addressed before, and they required adaptation of previous techniques. Since this line of experimentation is new, the pathophysiologic differences of awake and anesthetized models are also unknown. One model (macrosphere) was chosen to investigate these differences.

Awake models might be considered more realistic to human stroke. At the very least, awake models would limit the complications that surround anesthetized models. If the drawbacks of anesthetized models are related to the limited clinical impact that the research has had on stroke treatment, then awake modeling might allow for more directed intervention.

## 3. Methods

### 3.1 *Heart rate (HR)*

**T**wo electrodes are subcutaneously placed on either side of the chest just under the armpit. These leads are connected to a small amplifier and input into the data acquisition system. This channel is then used in a real time rate calculation that is then averaged over 5 seconds for smoother results.

### 3.2 *Femoral Artery Catheterization*

A lateral incision is made in the ventral aspect of the hind limb (usually the animal's left). Through this opening, the femoral artery and vein are located. The vein is the darker and larger of the two and it is usually found posterior and slightly ventral to the artery. The artery is isolated proximally and all connective tissue is removed for several centimeters of length. A distal ligature is attached using 3-0 silk. This is retracted as another suture is brought around the proximal aspect of the artery, however this suture is not tightened. Blood flow is stopped by retraction of the proximal suture and a small incision is made on the artery. Sharp forceps are entered into the hole and used to pull the artery wall around PE 50 (Intramedic, Beckton Dickinson) tubing that has been pre filled with heparinized saline and attached to a pressure transducer. The tubing is then advanced towards the heart several centimeters and the proximal suture is closed around the artery and tube. The ends of the distal suture are also

fastened around the tubing. In awake animals, this tubing is then momentarily occluded and disconnected from the transducer while it is passed through a subcutaneous tunnel that exits out the animals posterior just lateral of the tail. The wound is closed with 0 silk and the sutures around the catheter line are left loose to allow free movement.

### **3.3 *Cerebrospinal Fluid Pressure (CSFP) Measurement***

The 4<sup>th</sup> lumbar vertebra is palpated just above the hip bones, and a midline incision is made over the spinal cord. The fascia and musculature along the spinous process are severed and the spinous process is cut away. The resulting opening is cauterized and the remaining vertebra is carefully ground away with a surgical burr until the underlying dura is exposed. A small hole is made in the dura with an 18 G needle and a Tygon Microbore (.01" ID .03" OD, Saint-Gobain PPL Corp.) tubing is quickly inserted into the spinal canal. This tubing is filled with saline and connected to calibrated pressure transducer. The hole is sealed with cyanoacrylate adhesive and the patency of the catheter is verified by jugular compression which increases. The wound is closed with 0 silk around the catheter line.

### **3.4 *Electroencephalography (EEG)***

Two unipolar electrodes are placed subcutaneously over each hemisphere producing a right and left channel for EEG recording. These leads are then connected with the signal amplifier and input into two separate channels to the MP100. The signal is collected without Online filtering. Figure Q shows an

example right and left EEG recordings collected with the system in a restrained rat that was regaining consciousness.

### **3.5 Anesthesia Methods**

The different criteria for experiments required different anesthesia choices to fit the needs. For studies where the animal was to remain anesthetized during the preparation and experiment, a combination of Ketamine (80 mg/kg) and Xylazine (20mg/kg) was used. When the animal was prepared under anesthesia and is awakened under restraint a reversible agent was used. While Xylazine is reversible with Yohimbine, this reversal was not quite satisfactory in preliminary experiments. An alternative, medatomidine and its reversal agent, atipamizole was evaluated. Like Xylazine and Yohimbine, Medatomidine and atipamizole are adenergetic receptor agonists and antagonist respectively. However, medatomidine and atipamizole are much more selective to  $\alpha$ 2-adenergetic receptors and thus have a more specific action without pharmacologic interference.

Medatomidine and atipamizole are veterinary drugs manufactured specifically for use in dogs under the trade names Domitor and Antisedan (Pfizer animal health division). Once an appropriate dose was established, the drug was quite effective in rats. Full sedation was aided by a light dose of ketamine (10mg/kg) in conjunction with the Domitor (1mg/kg). This sedation was completely reversed within 2 minutes of an injection of Antisedan (5mg/kg). Figure G shows the physiologic changes in an animal that was given atipamizole to revive it from medatomidine anesthesia. The performance of these drugs was

adequate to prepare an animal under complete sedation, but then reverse this sedated state in order to conduct experiments on a fully conscious subject.

For one set of studies, inhaled isoflurane (1-2% delivered in O<sub>2</sub> at 1 L/min) was used to induce and maintain anesthesia. Reversal of this sedation was achieved by discontinuing the gas, and allowing the animal to regain consciousness. Sedation was easy to achieve and maintain and the reversal usually took from 5 to 30 minutes. Some complications arose during longer periods of anesthesia and several animals perished from respiratory failure. This problem was attributed to inflammation of the airway because of the dry anesthetic gas being inhaled at a high concentration.

### **3.6 *Pilot Stress Studies Methods***

Male SD rats (N=6) were lightly anesthetized, placed in the restrainer and then awoken for 90 minutes of restraint per day for 8 days. On the first, third, fifth, and eighth day the animals physiology was monitored, and blood was taken after the session via an eye bleed. Base line blood was also taken 3 days prior to the experiment and blood was taken after 10 minutes of exposure to isolated fox scent. The blood was assayed for corticosterone levels via a radioimmunoassay kit (ICN Pharmaceuticals). Physiologic data and corticosterone levels were tabulated every 10 minutes and all of the numbers were averaged for each day.

### **3.7 *Histology Methods***

During pilot studies, a method for visualizing the cerebral arteries was revised from Coyle and Feng (1993). Under anesthesia the heart was exposed

and heparin (1000 units) and papaverine (10 mg/kg) was injected intracardially. A syringe with a blunted 18 G needle was introduced into the aorta via the left ventricle and 15-30 ml of saline were flushed through the circulation followed by 10 ml of molding latex rubber. The brains were removed and fixed in formalin. This method allows for clear visualization of the arteries as seen in figure J.

For the macrosphere stroke studies, the brains were fixed by intracardial perfusion of 4% paraformaldehyde in phosphate buffered saline (pH 7.4) and postfixed over night. After storage in 40% sucrose the brains were sliced on a freezing stage microtome at 30  $\mu$ m. Two sets of 3 slices were kept at regular intervals (every 1.05mm) and transferred onto slides for later staining. The remaining slices were placed in cryoprotectant. For each 1.05mm there are two sets of slides representing the majority of the cerebrum. The first set of slides was stained with H and E stain and the second was stained with thionin.

Hematoxylin and Eosin staining was conducted by first rinsing and rehydrating the slices in 2 changes of tap water for 1 minute each. The slices were then stained in a 1:5 dilution of stock mercury free harris hematoxylin for 6-8 minutes after which the slices were rinsed for 3 minutes in running tap water. The slices were then placed in 1% acid alcohol (1000 ml H<sub>2</sub>O and 10mL con. HCl) to differentiate for 1 minute. This acid alcohol was rinsed with running tap water for 1 minute. The slices are then fixed in ammonia water (1000 mL H<sub>2</sub>O and 2-3 drops of 27% ammonia) until sections turned blue (10-30 seconds). This solution was rinsed for 5 minutes in running tap water followed by a 2 minute soak in 80% EtOH. Slices were then stained in 1:10 dilution of Alcoholic Eosin

(2g eosin, 160mL H<sub>2</sub>O, and 640mL 90%EtOH) and 80%EtOH for 2 minutes. Slices were dehydrated with one minute rinses in 90%, 95%, and 100% EtOH and cover slipped after 2 rinses of xylene.

For Thionin staining, the slides were rehydrated in phosphate buffer for several minutes and stained in Thionin diluted from stock 1:3 with PBS. After staining the slices were differentiated in 70% EtOH according to the desired level of contrast in the cells. Times for this rinse varied from 1-3 minutes. Slices were dehydrated and cover slipped according to the H&E methodology.

To calculate the lesion volume, in brief, first the over all area of each slice was determined by scanning in a slide of 3 representative slices and calculating an average area based on the complete slices present. This was calculated for all slices and each hemisphere. Then the lesion was traced by hand on the same slices. From these area measurements, the volume was determined by multiplying by the slice thickness and adding all of the values. The lesion volume was divided by the ipsilateral hemispheric volume to derive the percentage of the hemisphere that the lesion occupies (%HLV).

The scanning was carried out by illuminating slides with a calibrated light source and digitizing them with a Pulnix CCD camera and a Nikkor 90mm macro lens. This 256 grayscale image was input into a Macintosh G4 with an ATI rage video capture card. The images were evaluated in NIH image v1.62 in threshold mode that was calibrated for area measurement. The overall slice area was automatically calculated by setting the threshold low enough to include all tissue, this was 4 values above the threshold where the clear glass was included. The

total slice, ischemic lesion, left, and right hemispheric area was then calculated after these regions were circled with a cursor.

Several animals were used for pilot studies to outline the cerebral arteries system by latex casting. This was originally developed as a method to visualize obstruction in the arteries but gave us a good model for the visualization of the arterial system in the rat brain which is otherwise unobservable after normal perfusion fixation. Figure 1 shows an example of this technique.

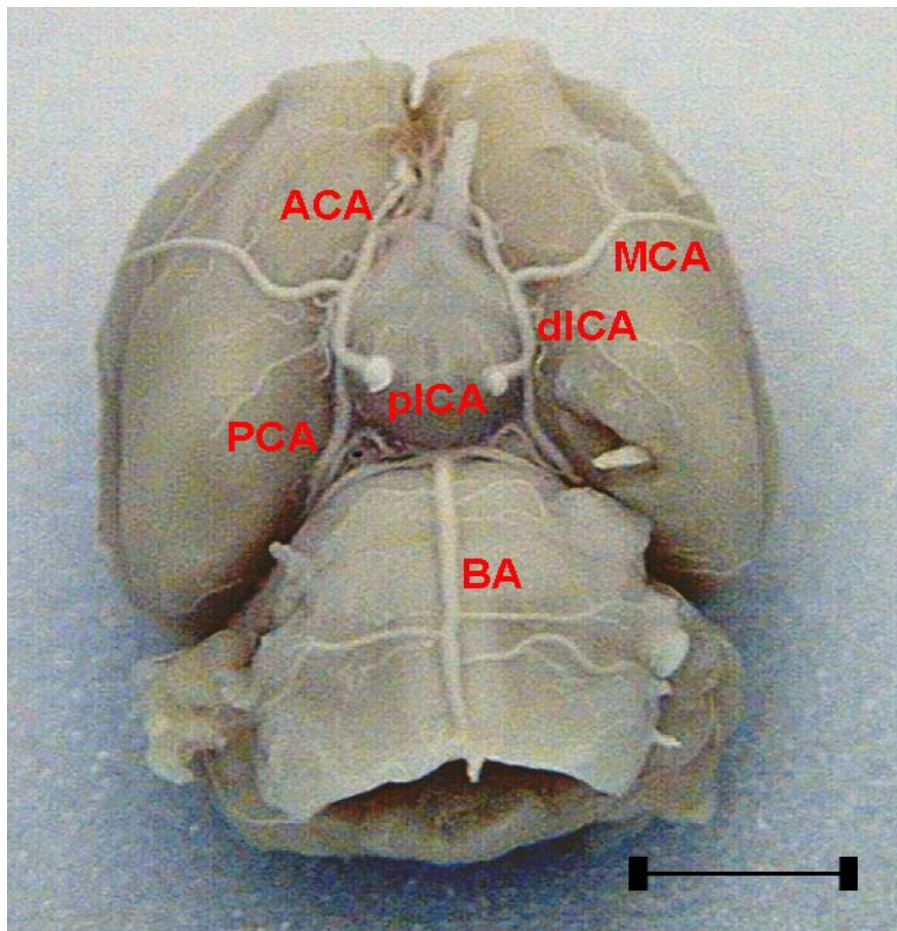


Figure 1: Latex impregnated cerebral arteries of the base of the brain. The major arteries are labeled as follows; ACA- anterior cerebral artery, MCA- middle cerebral artery, PCA- posterior cerebral artery, dICA- Internal carotid artery (distal portion), pICA- Internal carotid artery (proximal portion), BA- basilar artery. Bar equals 1cm.

### **3.8 Model Methods**

All models use male Sprague Dawley rats (Harlan SD) except for the SPSHR model. The size of the animal is very important since they need to be small enough to fit in the restraint apparatus but big enough to operate on easily. Animals around 300-350g were best for these studies.

#### **3.8.1 Suture SAH**

Through a midline neck incision the right common carotid artery (CCA) was dissected to the point of bifurcation. The external carotid artery (ECA) was ligated with 3-0 silk. The CCA was ligated several centimeters from the bifurcation and another ligature was placed loosely around the bifurcation. A small incision was made in the CCA and at this point the awake and anesthetized protocols deviated. In the anesthetized animal a 4-0 prolene suture was passed into the opening and the distal CCA suture was tightened around it but not to the point of binding it or inhibiting its advancement. This suture was then advanced to the bifurcation while the amount of suture left exposed outside of the CCA was measured for reference. The prolene suture was then advanced along the ICA until resistance was felt. This point was about 17–22 mm in from the bifurcation. Short, repeated “stabbing” motions were then used to breach the arteries causing a sharp rise in ICP. The prolene suture was withdrawn and the ligature was tightened fully to ligate the distal CCA after which the neck wound was closed.

In the awake animal, a specially designed suture-advancing catheter (Figure 2) was inserted into the CCA and attached to the artery with ligatures. Under visual inspection the suture was advanced while checking to insure that it

traveled down the ICA. Once the suture was advanced about 15 mm the advancement was stopped while the neck was closed and the catheter attached to the animals body with several loops of suture. Once the animal was placed in the restrainer and awoken, the suture was remotely advanced the remaining distance. Resistance was hard to gauge with this setup so the suture was advanced and retracted 5mm at a time in stabbing motions until a change in ICP was noted.

A remote suture advancing catheter was constructed as outlined in figure 2. The outer casing consisted of one short (10mm) section of PE 50 tubing connected to a 50 mm section of PE 260 which was connected to a 40 cm length of PE 60 tubing. The internal element was a 35 mm length of 4-0 Prolene suture attached via 5-0 silk knots to a 50 cm length of 1mm diameter nylon monofilament line.



**Figure 2:** Diagram of the catheter designed for inducing SAH in the bore of the magnet.

The components and lengths of each are; A- 4-0 Prolene suture (35mm), B- 5-0 silk binding, C- heavy monofilament nylon (50cm), D- PE 50 tubing (D<sub>1</sub> 10mm, D<sub>2</sub> 40cm), E- PE 260 tubing (50mm). The whole assembly is filled with petroleum jelly before the section D<sub>1</sub> is inserted into the CCA.

### **3.8.2 SPSHR Model**

The method for hemorrhage induction in SPSHRs is simple but requires the animals to be in a susceptible state for manipulation. The animals were weaned at 3-4 weeks of age onto a special stroke prone diet. Animals were checked about every 10 days for body weight and blood pressure. Litter mates were closely observed and when any member of the litter began to show symptoms of stroke, the others were used in experiments.

For the physiologic studies, the animals were anesthetized and underwent femoral artery and vein catheterization and trans lumbar intraathecal catheterization. They regained consciousness in the restrainer and allowed to equilibrate for 30 min. An IV injection (10 mg/kg) of norepinephrine (NE) was used to elevate the blood pressure in order to induce hemorrhage.

A simpler method that is not conducive to full physiologic monitoring, but can be repeated in the same animal and has been proven to work in the magnet (Brevard, 1999) is the percutaneous tail vein catheter. A PE 50 tube tipped with a 25g needle is inserted into the lateral tail vein and used to inject the dose of NE. This method can be used repeatedly if a trial fails to produce hemorrhage in an animal after MRI investigation.

### **3.8.3 ICH model**

The animal was placed into a stereotaxic head holder after it has been anesthetized. A midline incision was made on the scalp and the skull exposed near bregma. A hole was made in the skull 1 mm rostral, and 3 mm right of bregma and a 25 gauge catheter was lowered through this hole to a depth of 5

mm and cemented into place with cyanoacrylate glue. A Y fitting was attached to this catheter with 2 branches of PE 50 tubing filed with saline. One of the branches was open on the end, and the other was connected to a 100  $\mu$ l hamilton syringe. Once the animal was in the restrainer and conscious, .4 ml of blood was drawn from the femoral artery (see previous catheterization procedure). Blood was drawn from through the open branch of the PE 50 tubing and into the syringe. This open end was then sealed with a Hemoclip and 50  $\mu$ l of this blood was pushed into the caudate nucleus via the catheter at a rate of 25  $\mu$ l per min.

#### **3.8.4 Macrosphere Model**

Anesthesia was induced and maintained with 1-2 percent isoflurane in oxygen delivered at 1L/min. The left femoral artery was exposed and catheterized for recording of blood pressure and sampling of blood before, and after occlusion for blood gas analysis. After closure of the incision, the common, external, and internal carotid arteries were exposed via a midline neck incision. The ECA was isolated, and the superior thyroid, the pterygopalatine, and the occipital arteries were ligated with a 5-0 suture.

Six TiO<sub>2</sub> spheres of 0.3 to 0.4 mm in diameter (BRACE GmbH, Alzenau, Germany) were suspended in heparinized saline in a length of PE 50 tubing. This tubing was inserted into the external carotid artery which was previously dissected and ligated. During the arteriotomy the CCA and ICA were temporarily ligated with two 3-0 sutures to avoid excessive bleeding. The tubing was advanced to the carotid bifurcation but was not advanced to the point that it

would block blood flow from the CCA to the ICA. This tubing was held in place with a 5-0 suture. Once in place the tip of the catheter was adjusted to allow efficient flow of the spheres into the ICA.

In the awake group, the tubing was passed through a subcutaneous tunnel made from the xyphoid to the neck incision. The tubing was then fixed with ligatures at the entrance into the skin, and periodically around the body so that the tubing was fixed to the animal. The neck incision was then closed with 0 silk. In the anesthetized animal, the incision was left open until after the sphere injection. All of the animals were then fitted with sensors and monitored for blood pressure, pulse oximetry, temperature, respiration rate, and EKG.

The animals in the awake group were placed into a special restraining device (Insight Neuroimaging Systems LLC, Worcester MA) while still sedated. After restraint the animals were allowed to regain consciousness by removing the isoflurane gas. The anesthetized group remained prone for the injection of the spheres and closure of the incisions, after which time they were lay on their side.

The macrospheres were introduced slowly into the ICA in small bolus injections of heparinized saline where they were carried into the cerebral arteries by the blood flow into the cerebral circulation. After the macrosphere injection, 0.5 ml of heparinized saline was injected into the ICA to flush any remaining spheres into the circulation. Before closure of the anesthetized groups incision, the tubing was removed from the ECA which was then ligated with 5-0 silk.

The animals were observed and monitored for a 90 minute period following embolus injection. At 60 minutes a small blood sample was taken and

analyzed. Anesthesia was discontinued in the sedated group and the animals were allowed to regain consciousness in their cages. The animals in the awake group had their catheters ligated next to the skin with Hemoclips (Weck Closure Systems). They were then carefully removed from the restrainer and returned to their cage to recover.

All of the animals were observed for the next 3 hours during which time they underwent neurological scoring and temperature measurement. After 24 hours, another neurological score was taken along with the animals temperature. The animals were then sacrificed and the brain was fixed.

### **3.8.5 Suture MCAO Method**

Briefly, the neck was exposed as mentioned in the macrosphere method. Prolene (Ethicon) nylon suture (4-0) was blunted with heat and coated with silicone. This suture was then introduced and advanced through an arteriotomy in the ECA while the CCA and ICA were temporarily ligated. Once the suture was loosely secured with 5-0 silk, the ICA ligation was removed and the occluder was advanced into the ICA until 16-18 mm of its length lay beyond the carotid bifurcation. This was often the point of slight resistance when the occluder tip had lodged in the ACA. Once the occluder was in place it was fixed with a 5-0 suture and the CCA ligation was removed.

### **3.8.6 Photothrombosis Method**

Animals were anesthetized with pentobarbital (50 mg/kg). The scalp was incised to expose the skull surface. Rose Bengal (10 mg/kg) was injected into a

lateral tail vein while a fiber optic light guide transmitted light from a 100 watt mercury vapor light source (Zeiss Optical) directly to the skull surface. This light remained on for 5 minutes after which time the animals scalp was sutured closed and treated with lidocaine and betedine. The animal was returned to its cage. Seven days later the animal was sacrificed and its brain was removed and immersed in 10% formalin for 1 month.

### **3.8.7 Neurologic scoring**

Neurologic examinations were performed 2 and 24 hours after MCA occlusion based on a system derived by Longa et al (1989). The neurologic findings were scored on a 5 point scale; 0- no neurologic deficit, 1- failure to extend a forepaw fully, 2 -circling to the left, 3-falling to the left, 4 -not walking spontaneously with a depressed level of consciousness, and 5-deceased.

### **3.9 Statistics**

Comparison between the before and after stroke variables was conducted by using a paired t test. For comparison among the cohorts, the physiologic and histologic measures were compared for significant difference using a Kruskal-Wallis test, a nonparametric analog of ANOVA. Variables with significant difference were analyzed with Dunns test for nonparametric multiple comparisons. Paired T Tests were used to analyze significant deviations of the blood corticosterone levels from baseline for the stress acclimation study.

# 4. Results

## 4.1 *Physiology System*

In order to carry out physiologic measurements within a MRI scanner, a compatible monitoring system had to be developed. The physiology system consisted of a number of sensors and peripheral amplifiers that were each connected to a central analog to digital converter interfaced to a PC that was running data acquisition software. The converter and software were purchased from Biopac Systems (Model MP100). Each of the peripheral components were purchased separately and each input to the data acquisition system via a separate channel for each parameter. The MP 100 unit was configured to collect 200 samples per second for each channel. This data often consumed about 10 megabytes of disk space per hour of data collected. Figure 3 shows a sample of physiology measures that were taken with noninvasive probes. The system consisted of:

- EEG/EKG amplifier
- Fiber optic Pulse Oximeter
- Pressure transducers
- Temperature Probe
- Piezo electric sensors

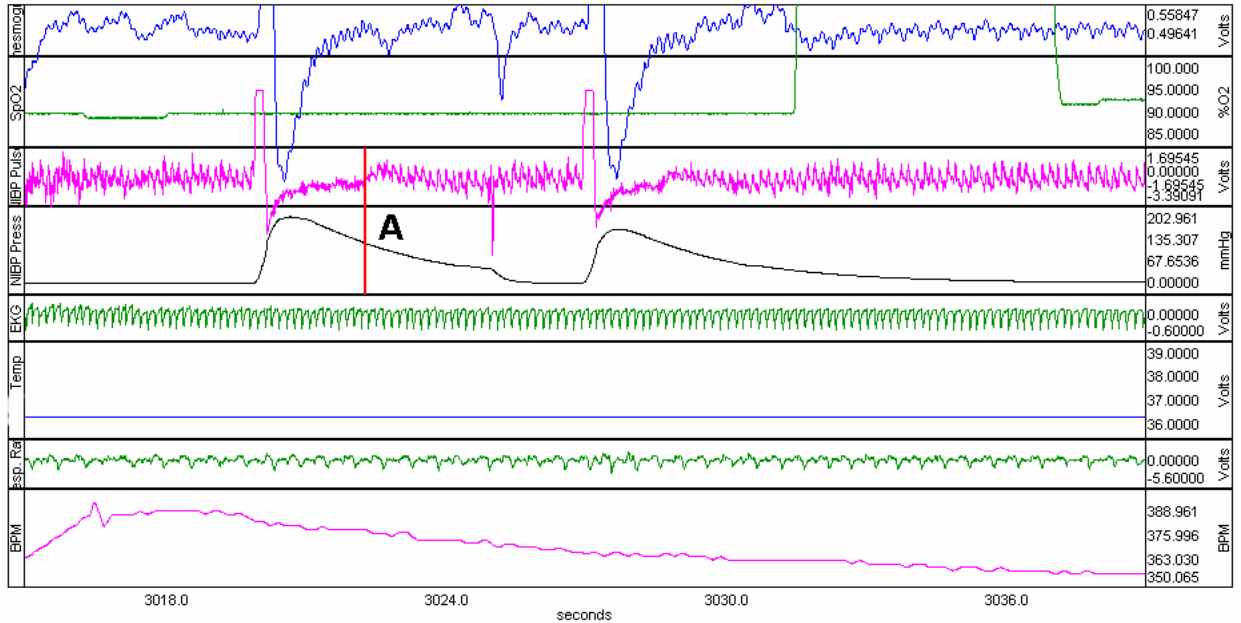


**Figure 3:** A sample physiologic trace for an animal in the MRI restrainer using only non invasive sensors. The top trace is the pulse waveform from the infrared pulse oximeter. The next trace (SpO2) is the partial pressure of oxygen at the skin, also from the pulse oximeter. The 3rd channel is the pulse sensor on the tail. The signal is lost when the pressure cuff is inflated and returns at the systolic pressure equivalency point (red line labeled A) on the pressure curve (4th channel). The 5th channel is the raw EKG wave form, while the 6th is the core temperature. The 7th channel is the respiratory wave form from a thoracic pressure sensor, and the 8th is a calculated heart rate per minute from the EKG signal.

A Nonin Model 8400v pulse oximeter was purchased with a fiber optic sensor and cable. This unit measures the percentage of oxygen at the skin, SpO<sub>2</sub>%, and provides a plethysmographic pulse waveform, derived from an infrared light source, from which heart rate (HR) can be measured. A cable was

made to output the data from the machine to the data acquisition system based on the product specifications supplied by the manufacturer.

The performance of the pulse oximeter was dependent on blood flow to the extremity to which the sensor was attached. The limbs provided the best source, but often the sensor became detached from an awake animal as it kicked. The tail provided a good alternative for placement. The drawback to placement on the tail was that the blood flow to the tail is very inconsistent and can be altered consciously, or automatically depending on temperature and stress. Low temperatures in subject animals often caused a diminished signal that was not usable.

To measure the blood pressure invasively, a femoral artery catheter was used. In an anesthetized animal, it is a straight forward procedure to place and retain the catheter. Awake animals added a unique dimension to the effective use of a femoral artery catheter. Sudden and strong movement by the animal often led to the catheter becoming dislodged, at which point death was almost certain. In several trials, movement also caused the catheter to be blocked as it was pushed against some part of the animal's interior. Careful retraction of the tubing sometimes solved this problem, but was generally avoided because of the risk of pulling the catheter out of the artery. One strategy to compensate for these problems was to allow the catheter to pass out of the body without attaching it to anything that might be pulled against the artery such as a muscle or the skin.

The pulse wave form from a direct arterial catheter relayed an accurate heart rate so long as the patency of the catheter was maintained. Because of the

invasiveness of putting in an arterial catheter, this was not a common method for HR measurement, however.

The blood pressure was derived non invasively (NIBP) from the tail of an animal via a sphygmomanometer similar to what is used on a human arm. A unit from Kent Scientific (BP 100) was acquired that consisted of an inflatable pressure cuff with a pressure sensor and a pulse sensor. Both of these sensors were plugged into signal amplifiers that then input into the data acquisition system. Figure 3 shows a sample of two BP measurements. The NIBP pulse channel loses the pulse as the tail is occluded. After the pressure begins to fall, the pulse reemerges, and the pressure can be read from the NIBP press channel at that point.

These sensors were placed on the tail of the rat and relied on the occlusion of the pulse in the tail to determine the systolic pressure. When taking these measurements it was important that the animal remain calm with a normal core temperature. As with the pulse oximeter, insufficient flow to the tail diminished the signal to the point that it couldn't be used. This reduction was precipitated by stress. Figure 4 shows an instance where the experimenter entered the room at time "A", causing stress to the animal, which promptly reduced the blood flow to its tail and thus decreased the tail pulse. Often times, "priming" the tail by subjecting it to several short periods of occlusion would stimulate blood flow into the tail when flow had diminished.

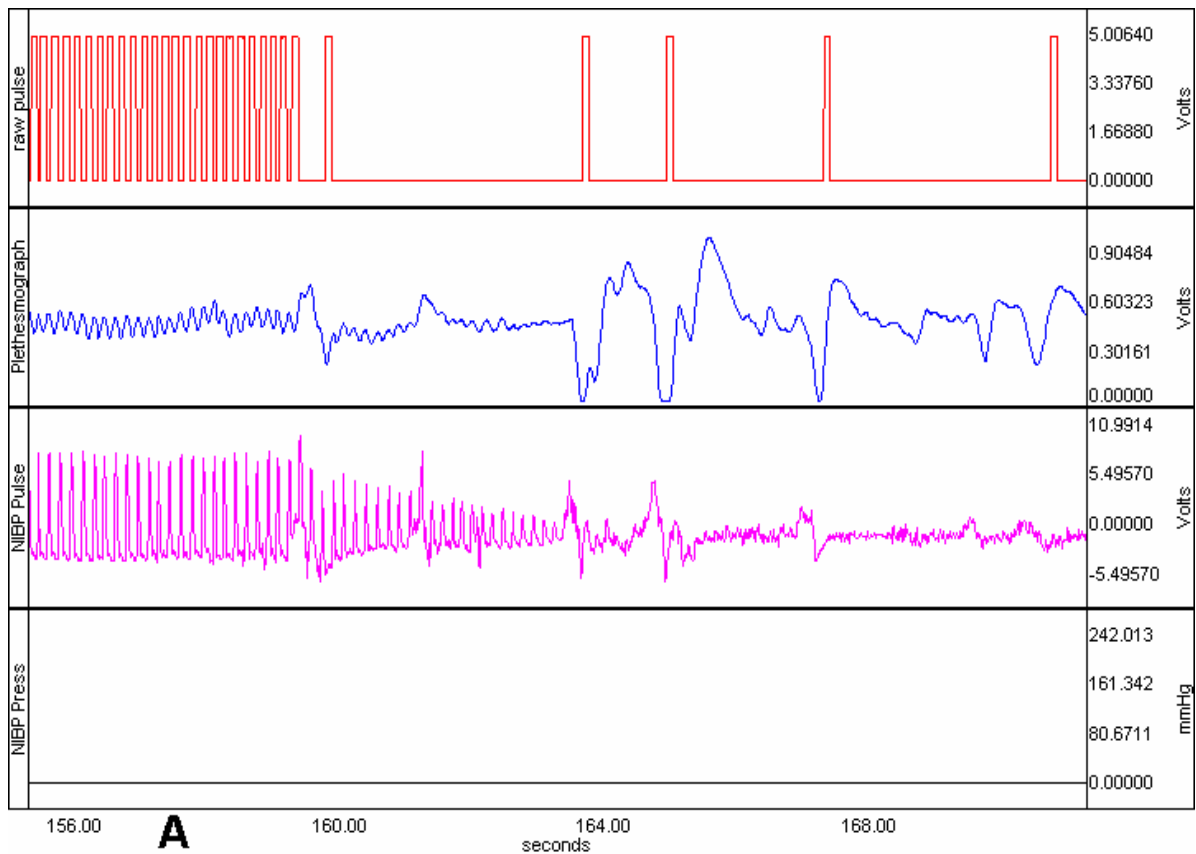


**Figure 4:** Entering the room during BP monitoring affects the tail perfusion in rats. The experimenter entered the room to monitor the animal at time point A. Subsequently, the animal reduced the blood flow to its tail in anticipation of inflation of an occluding cuff around the tail. With this reduction in blood flow, movement and respiration cause more of the changes in the circulation than the heart rate, and these artifacts can be seen in the plethysmograph channel.

Heart rate was derived from several sources in the system. Real time rate calculations made by the Biopac system allow heart rate to be calculated from the pulse wave form that the Pulse Ox generates, from the tail pulse sensor on the NIBP sensor, from the EKG signal or from the pulse wave form in the invasive blood pressure measure. The EKG provided the most consistent source

for calculating the rate (the 8<sup>th</sup> channel in figure 3). Both the NIBP tail sensor and the pulse ox were reliant on the circulation to the extremities and therefore, did not always provide consistent data for HR determination. When proper circulation was achieved, the wave forms were sufficient for accurate HR measurement.

The placement of a force transducer on the chest of the animal provided us with a measure of respiration rate (RR). The signal (the 7<sup>th</sup> channel in figure 3) varied in amplitude. This made real time calculation of the RR fairly difficult for the software. When the animal was in a restraining tube, the sensor could be kept in close proximity to the thorax, and had a solid backing to provide a good signal. When the sensor was merely placed under the animal, the sensor would not provide such a strong signal. Because of the high sensitivity of the sensor, the signal was often accompanied by a great deal of noise from body movement and cardiac activity. These factors were the major reason that the RR signal had to be evaluated by a person in order to assess the actual rate.

One positive side effect of the high sensitivity of the force transducer was the presence of a large amplitude signal whenever the animal moved. These movements could then be counted to quantify the struggling activity of the animal during stress tests.

An MRI compatible method for measuring ICP had to be devised for these experiments. The clinical norm is to implant sensors directly into the skull of the patient. Fiber optic, implantable transducers and fluid lines are placed within the skull either epidurally or ventricularly so as to record pressure directly. Several drawbacks occur with these methods; for instance, the implantable components

are often larger in scale as they are for human use and the equipment is generally costly. The primary drawback is that this equipment requires a direct interaction with the brain, which can be pathologically damaging. This adds neurological and histological complications to stroke studies so it is favorable to look at methods that work more peripherally to the brain.

Two simple and common methods fit this criteria. Both cisterna magna and trans lumbar intrathecal catheters are simple, inexpensive procedures that do not directly alter brain pathology. The former was tried according to Barth et al. (1991) methodology. After pilot trials, however, the latter was chosen as a slightly easier procedure that had the least interference with the CNS. Little has been documented on this method, so a protocol was developed using the work by Jamali et al. (1998) as a guide line. This method is favorable because it is fairly quick and consistent and it uses MR compliant components. Once implanted, the catheter can be used for several days. Blood clots can compromise the patency of the catheter during a hemorrhage, but this was not an issue in the course of these studies.

The intrathecal catheter for measuring ICP gave us a reliable and accurate reading of CSFP. The sensitivity of this method is demonstrated in Figure 5 where the wave included both respiratory and cardiac wave components. Also, the patency was readily testable by jugular compression. Measuring a low pressure hydrostatic system with a fluid line and a pressure transducer made the system susceptible to interference from motion, but these artifacts were always transient. Because the system was working at a low

pressure it is very easily affected by changes in transducer or subject elevation. Therefore, the pressure transducer should always be kept at the same height as the animal to achieve an accurate baseline measurement.

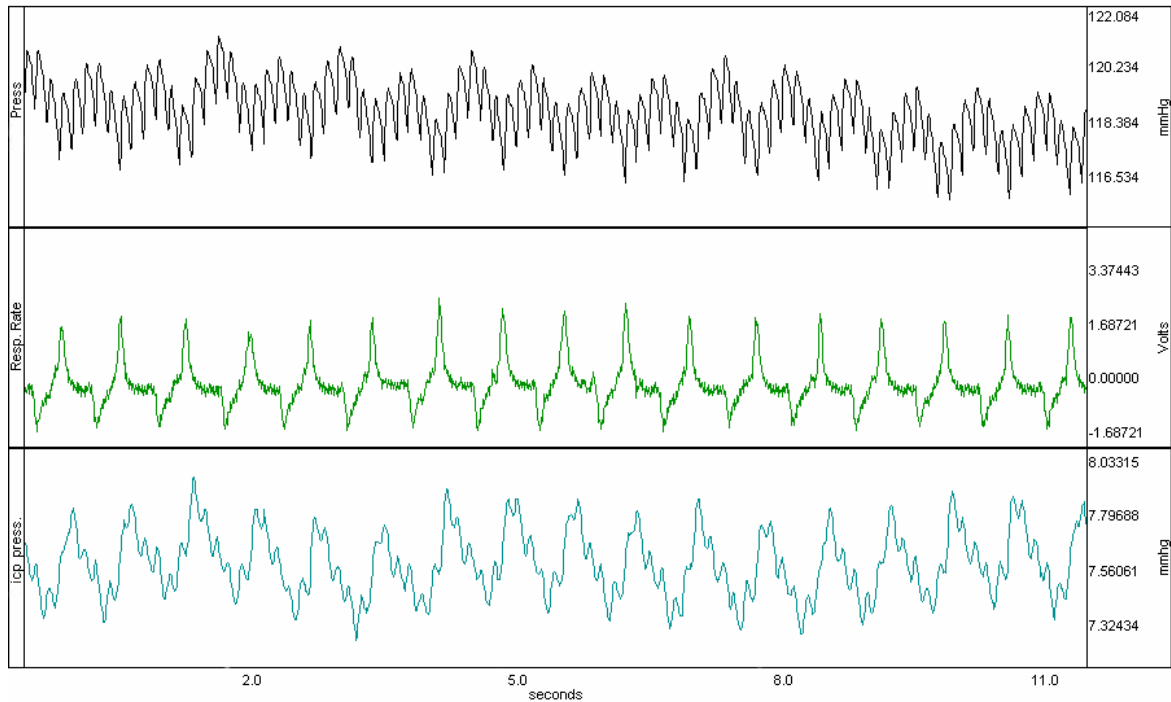


**Figure 5:** Direct blood pressure, respiration rate, and intracranial pressure waveforms.

The close up of the ICP wave form (bottom channel) shows circulatory and respiratory components that correspond well to the other traces.

EEG systems that work within an MRI environment are not commercially available. John Ives (1993) worked to overcome the problems inherent when simultaneously using MRI and EEG equipment, so this author was contacted and provided us with a system that he custom built for our application. Silver electrode wires, placed subcutaneously, are connected to a small preamplifier/multiplexor. These components and their power source have minimal ferromagnetic content to limit artifacts in MRI images. The multiplexed

(encoded so that multiple channels of data can be carried in one signal) data is then converted to a fiber optic signal to be sent outside of the magnetic field without interfering with it. The signal is then demultiplexed back to the original channels and input into the data acquisition system. Figure 6 shows the output of this system for a left and right set of electrodes as the animal emerges from anesthesia.

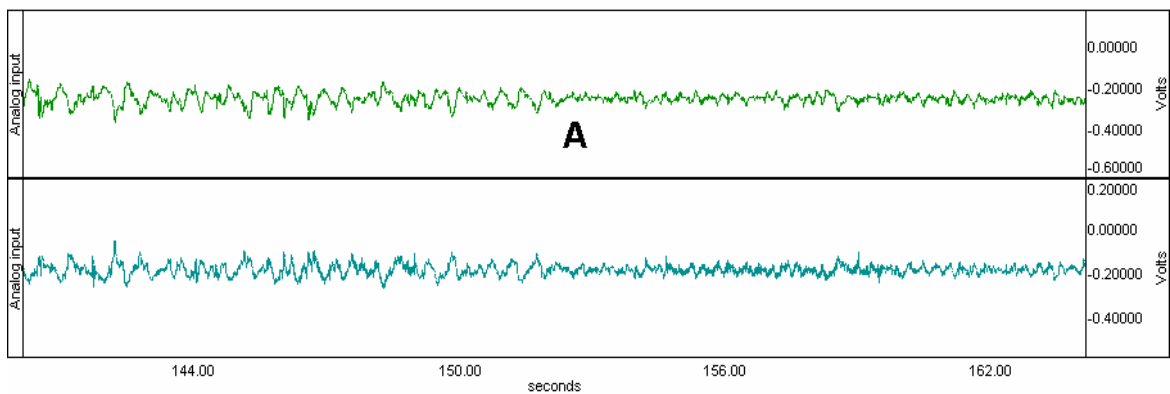


Figure 6: A sample EEG trace in an animal waking from anesthesia. Point A indicates when the wave form changes from theta to alpha waves. Right and left hemisphere activity are recorded in the upper and lower channels respectively.

The core temperature was measured with a rectal probe thermistor that was amplified and measured by a temperature controller (Cole Parmer). This controller then input into the data acquisition system. It also served as a feed back regulator to a supplemental heating system to maintain the animal's core temperature.

## **4.2 Anesthesia**

Restraint and preparation of an animal is often conducted with the aid of anesthesia. We tested several anesthetics that were reversible, so that after set up the animal could be awoken for study. Several adverse reactions were noted with different drug combinations. Most notably, Xylaxine and Etomidate both interacted negatively with norepinephrine.

Both of the reversible anesthetics that were used worked well. Medetomidine was quite effective for inducing sedation, and atipamizole never failed to reverse that sedation. Figure 7 shows the physiologic profile of a medetomidine sedated animal for 2 minutes after an atipamizole injection, while figure 6 shows an EEG trace of a similar animal as it wakes up. After experimenting with a dosage it was determined that 1mg/kg was sufficient for consistent medetomidine anesthesia with 33% of this dose for redosing. Isoflurane was more variant in the depth of anesthesia it maintained, but it seemed that the restraint stress helped to expedite recovery once the gas was discontinued.

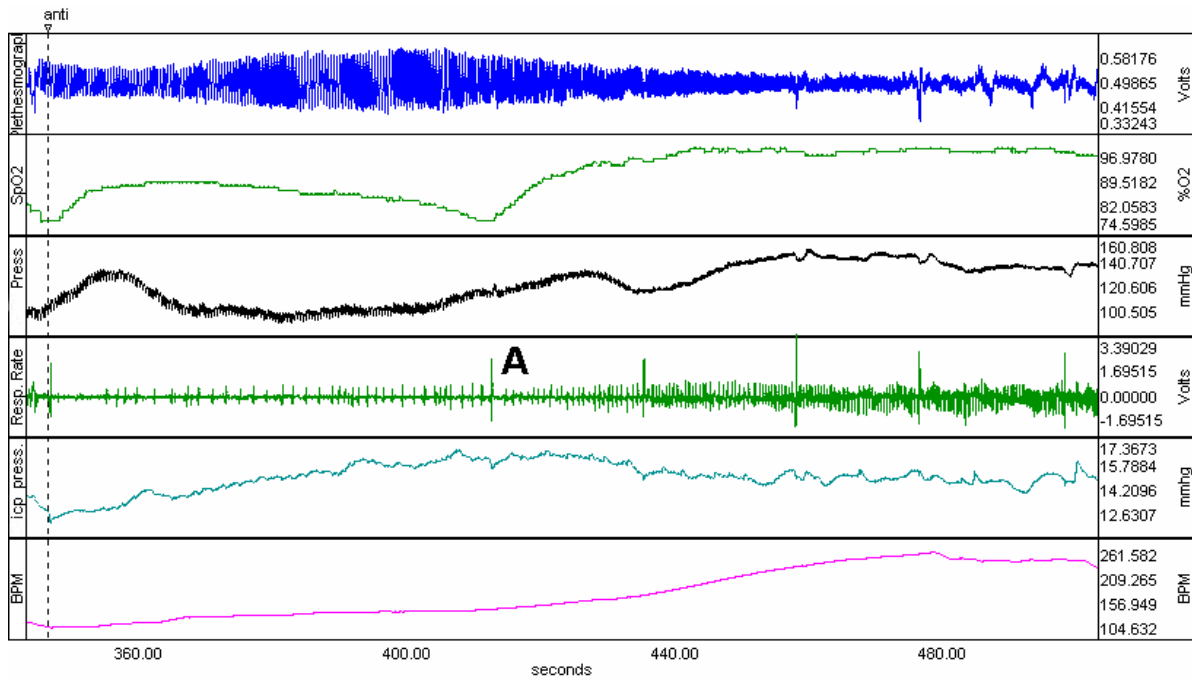


Figure 7: Effects of atipamazole on a medetomidine anesthetized rat. Atipamazole was injected at the time indicated by the dotted line. From the traces it can be seen that emerging from medetomidine anesthesia causes increase in the heart rate, blood pressure, respiration rate, ICP and SpO<sub>2</sub>%. The graph encompasses 2 minutes of time. From the spikes on the respiration rate channel (4<sup>th</sup>) one can see, at point A, that the animal's first movement was about one minute after atipamazole injection.

#### 4.3 Pilot Stress Study

Conscious restraint can cause stress in an animal, so stress levels were quantified by physiologic and biochemical means to assess if habituation to restraint could lessen the stress. Animals were subjected to 90 minutes of restraint, every day for 8 days. Heart rate and respiration were quantified every 10 minutes and all values were averaged for all animals for each day. Struggling movements were quantified for each 10 minute block and averaged for all

animals each day. The cortisol levels were measured from blood serum collected at the end of acclimation on day one, three, five, and eight.

The measures indicate a reduction in the animals' stress level over the course of the study. The heart rate and respiration rate diminished over the study indicating that the autonomic response to the restraint stress was lessened over the course of several sessions. Reduced levels of corticosterone indicate this decreased stress level. Important to the methodologies, the struggling movements of the animals diminished after 5 days of restraint sessions. Figure 8 shows graphical representation of this data.

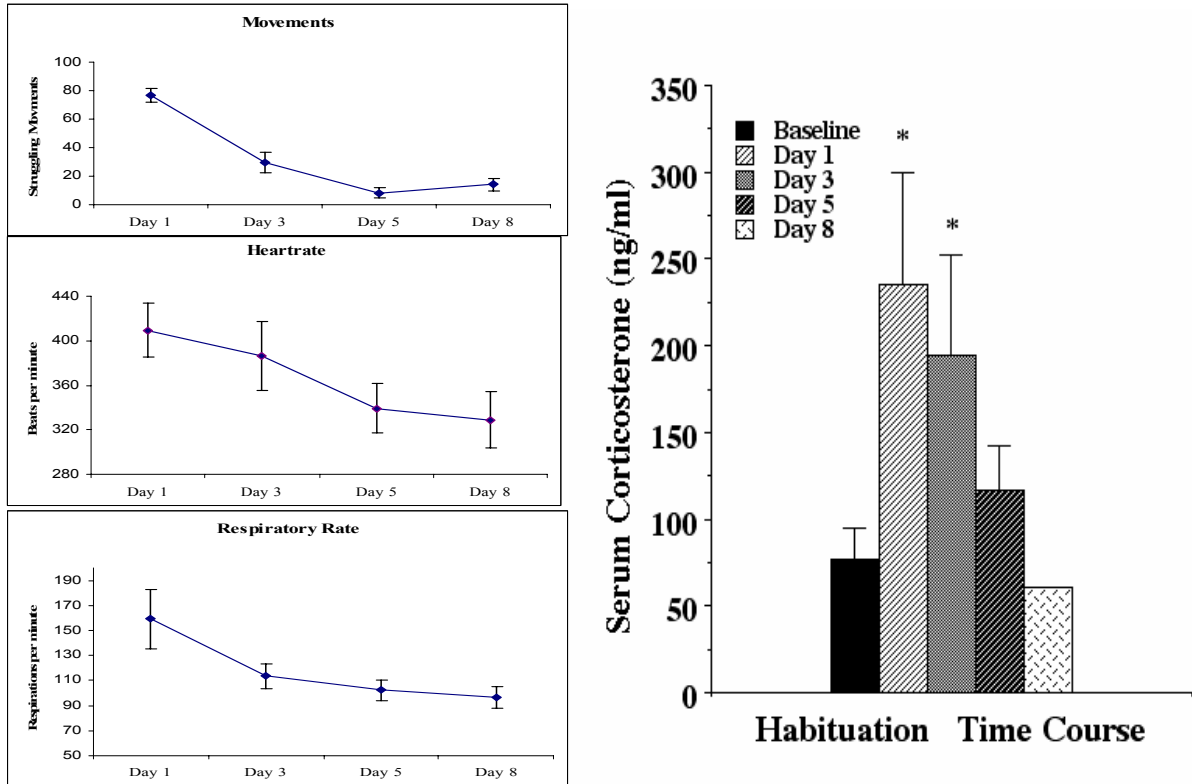


**Figure 8:** Acclimation of animals (n=6) to restraint stress over the course of daily restraint. These data show the normalization of physiology in conscious animals for 8- 90 min restraint sessions. The top left graph indicates that struggling movements decrease in the first 3 days of restraint and continue to diminish until day 5. The middle left shows a marked decrease in average heart rate for all 6 rats while the bottom left shows a decrease in respiration rate. The blood corticosterone levels diminish achieving normal levels by day 8 as seen in the right graph. The \* indicates significant changes from baseline as determined by paired T-tests ( $p < .05$ ).

#### 4.4 Models

Four models of stroke induction were successfully adapted to use in awake animals including spontaneous hemorrhage, intracranial hemorrhage,

subarachnoid hemorrhage, and macrosphere occlusion. Physiologic monitoring of each of these models was carried out during the stroke, and pathology was evaluated post mortem. The anesthetized suture MCAO and photothrombotic models were also studied.

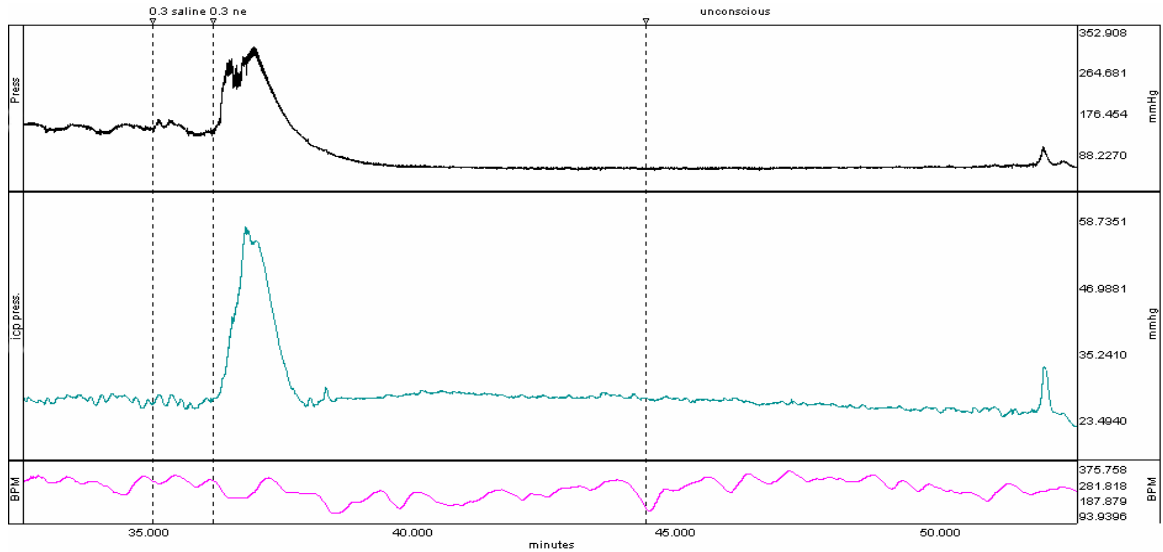
The hemorrhagic models were studied briefly for their feasibility in awake animals. The numbers of animals used for each group was not large enough to be statistically significant. Therefore, no conclusion about the differences of awake and anesthetized animals could be drawn. Also, only gross histology was evaluated on a qualitative, but not quantitative level.

The macrosphere and suture MCAO models were studied in depth. Awake and anesthetized macrosphere cohorts, and sedated suture animals were studied in statistically relevant numbers to investigate the effects of anesthesia. Detailed, quantitative histology was performed post mortem.

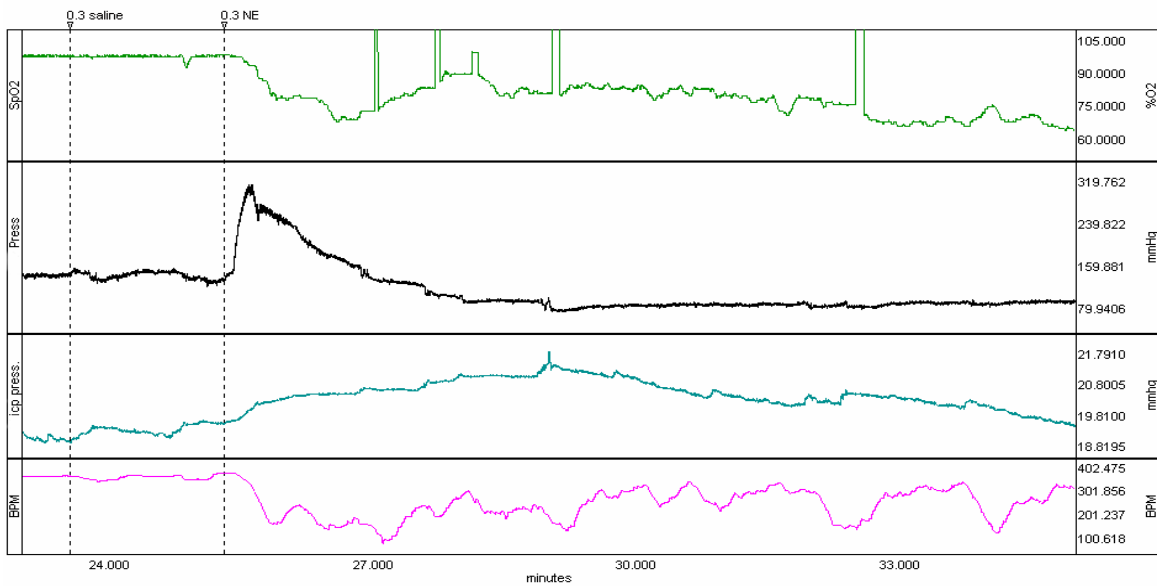
#### **4.4.1 SPSHR model**

To evaluate the physiology of SPSHRs during stroke, it was hypothesized that animals that were vulnerable to stroke could be induced to hemorrhage by injection of norepinephrine to increase BP. First trials were done with animals that were within the vulnerable age of 15-20 weeks as determined by previous work (Smead, 1989). None of the 5 animals experimented on showed any physiologic or postmortem signs of stroke. Animals were then deemed vulnerable when littermates began to stroke regardless of age. After one animal died of stroke, three cage mates from the same litter were experimented on and one animal had an acute rise in ICP that correlated to an acute rise in MABP. The

control animals had an equally extreme increase in MABP, but no appreciable change in the ICP. (figure 9) The brain of the animal that stroked was lost before stroke could be confirmed post mortem.



### Experimental



### Control

**Figure 9:** Physiologic parameters on a SPSHR model of induced hemorrhage and control animal. The upper trace shows an acute rise in ICP that coincides with the

elevation of BP. The lower trace is the effect of Norepinephrine on a control animal that did not stroke. Note the different scale of the ICP trace for each animal.

#### **4.4.2 SAH Model**

Achieving SAH in an anesthetized animal was very straightforward. Performing an SAH in an awake animal required a remote device to advance the suture after the neck was closed. A suture running through a piece of PE tubing was determined to allow adequate movement of the suture to introduce it into an artery, and further experiments demonstrated that petroleum jelly could be used to seal the tube from blood leakage while still allowing passage of the suture.

Induction was successful in 3 animals, one awake and two anesthetized. The characteristic physiology of one of the anesthetized animals is shown (figure 10). Post mortem inspection of the brains indicated SAH by large, extra-parenchymal deposits of blood (see figure 11). The remaining two animals both had lost the patency of their intrathecal catheter so the physiologic data could not be used.

Many sources have reported an acute rise in ICP after SAH induction that plateaus for several minutes at pressures near MABP. Figure 10 shows a similar reaction in this study. During the plateau, a small increase in MABP can be seen at point B that increases the BP to be greater than the ICP, possibly in an attempt to restore CPP.

Smaller sutures cause a more realistic stroke by lessening the interference that the suture has in blood flow through the artery (Schwartz, 2000). It has been seen in these experiments that hemorrhage usually does not occur

until the suture has been retracted. In figure 10, the artery was perforated at the second vertical dotted line; however, hemorrhage did not occur until the suture was retracted a short while later (A).

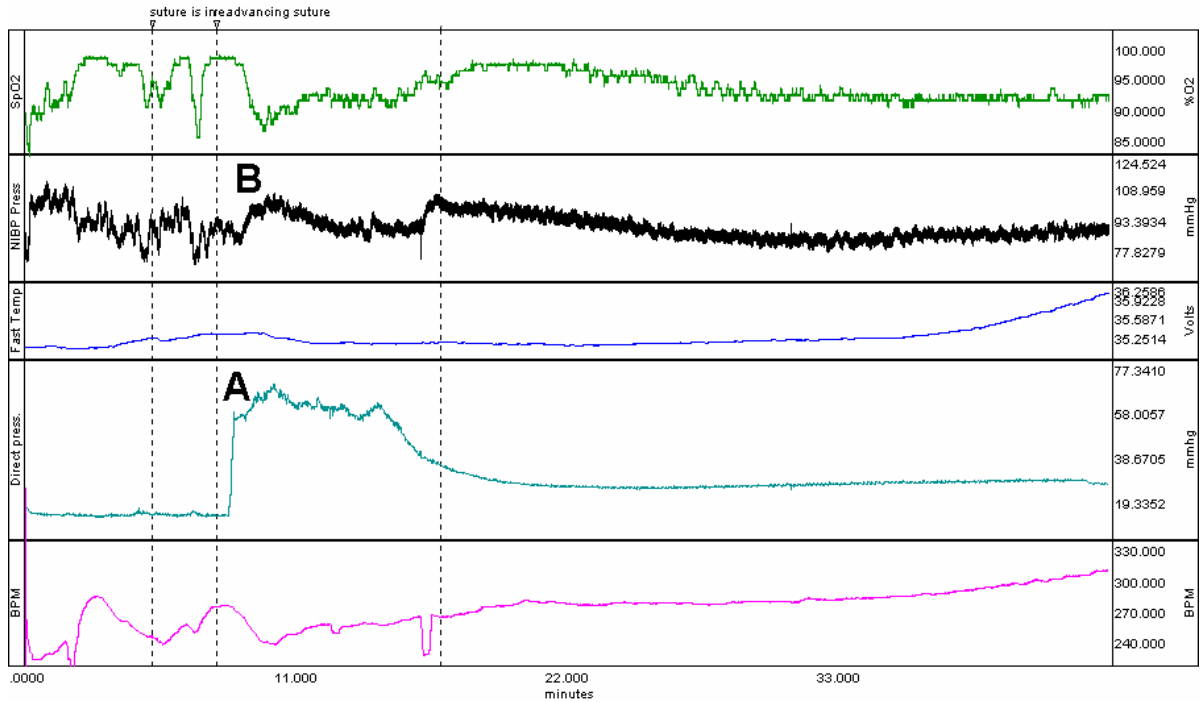


**Figure 10:** Physiology trace of a SAH in an anesthetized rat. ICP (channel 4) increased acutely at the point of hemorrhage (A), where it maintained an elevated level nearly equal to the MABP for 5 minutes. During this plateau, the MABP increased slightly at point B. After 5 min., ICP diminished, but did not return to baseline levels. The animal in this instance expired after several hours.

All of the animals were in poor condition after the stroke; they were hardly ambulatory and would only move if provoked. Death occurred within 2 hours of the hemorrhage. Large amounts of blood were found clotted in the extraparenchymal space as can be seen in Figure 11.

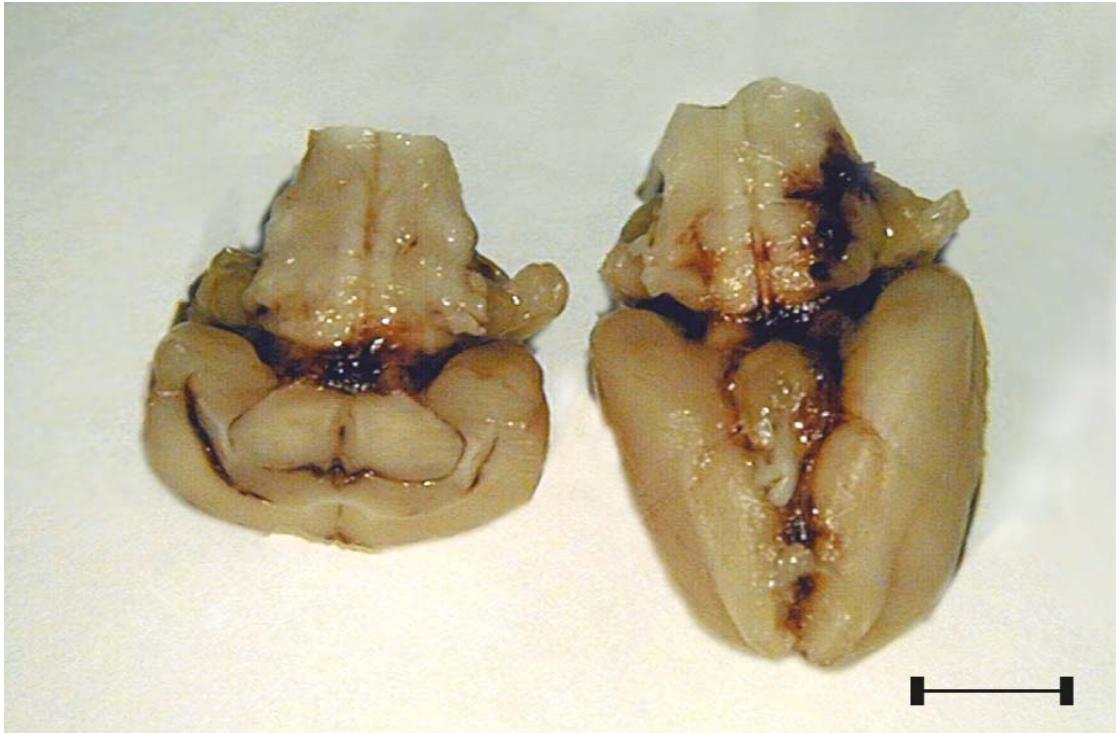


**Figure 11:** Postmortem condition of the brain after SAH induction. The brain on the left has been sectioned to show ventricular bleeding. Note on the right brain the lateralization of blood primarily to the animals left side. In this case this was the side of induction. Bar is equal to 1 cm.

#### **4.4.3 ICH Model**

Methodologically, the ICH is a simple model, even in awake animals. A catheter was placed into the brain, usually in the caudate nucleus, and blood was injected into this catheter shortly after it was withdrawn from an arterial line elsewhere in the body. From previous work it was determined that 50 microliters of blood should be injected into the caudate nucleus at a rate of 25  $\mu\text{l}/\text{min}$ .

Placement and use of the catheter was simple and the entry point of the catheter was relatively small and minimally invasive (arrow in figure 12). After the injection, the clot formed in the caudate nucleus and blood spread into the

ventricles. These strokes were severe, and the animals were sacrificed several hours after the stroke.

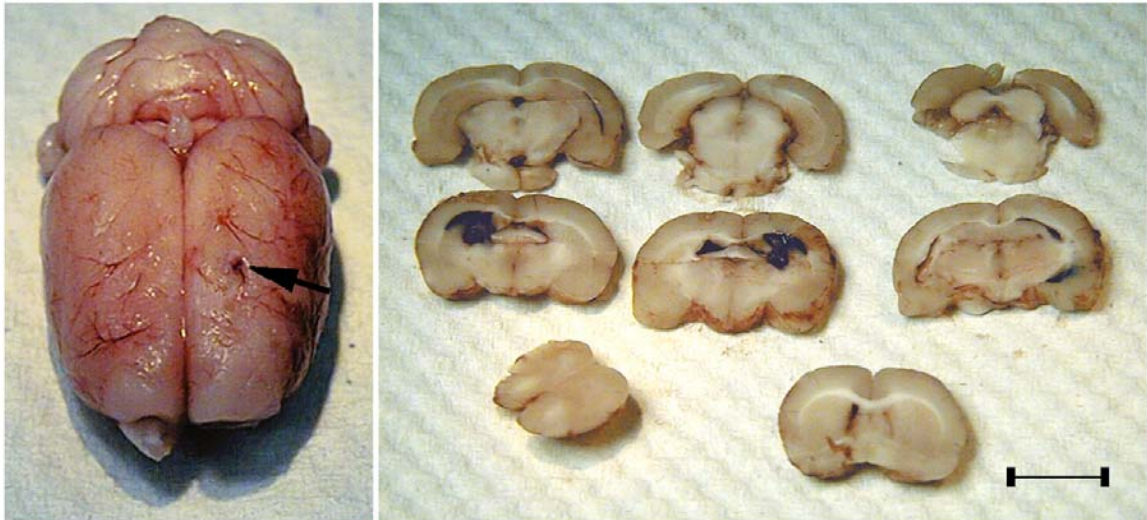
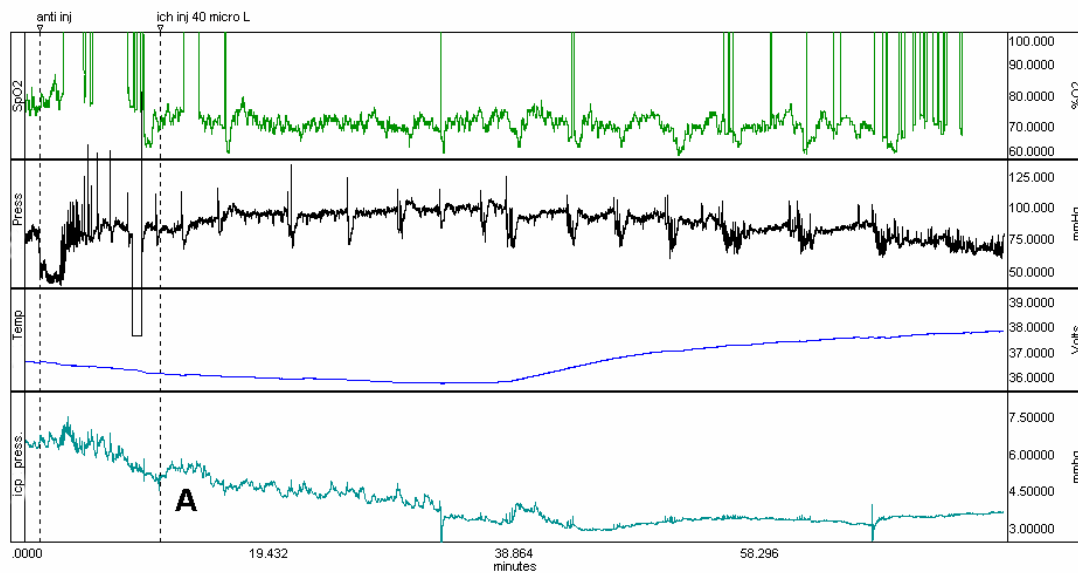
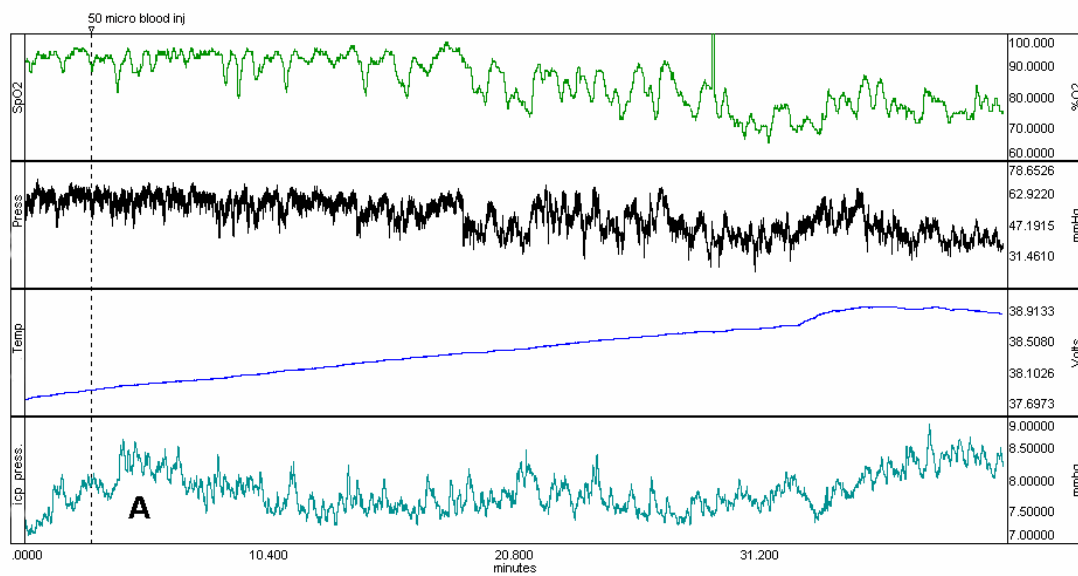


**Figure 12:** Brain and slices of ICH induction. The arrow indicates the point of entry of the cannula. Blood can be seen in the slices at the point of injection and in the ventricles. Bar equals 1 cm.

While ICP increases after ICH, these ICP changes are not large enough to affect CPP (Nath, 1987). In both the awake and anesthetized cohorts, there was a small, transient rise in ICP on the order of 1-2 mmHg. Figure 13 shows a trace of both an anesthetized (lower) ICH induction and an awake (upper) induction. The ICP increases that are labeled (A) are not sufficient to affect the CPP.



**Awake**



**Anesthetized**

**Figure 13:** Physiologic parameters of sedated and awake preparations of ICH. The upper trace is from an awake animal while the lower trace was taken in an anesthetized animal. The dotted lines are labeled for the time of injection and subsequent increases in ICP are labeled (A).

#### 4.4.4 Photothrombosis Model:

The feasibility of using this method was examined and Dr. Watson was consulted with on the design of the apparatus needed to conduct our studies in an awake animal within the MRI. Several bench top trials were made after developing a protocol. The brain from one of these trials shows an obvious lesion on the cortical surface (figure 14, A). Because of the relatively low power of the light source, the lesion is fairly shallow on the cortical surface (figure 14, B).

After several initial trials, using two anesthetized animals, it was determined that this method could not be easily carried out within the restraining apparatus in conscious, restrained rats within the MRI machine. Instead of purchasing the costly equipment needed to conduct these experiments, this method was abandoned all together.

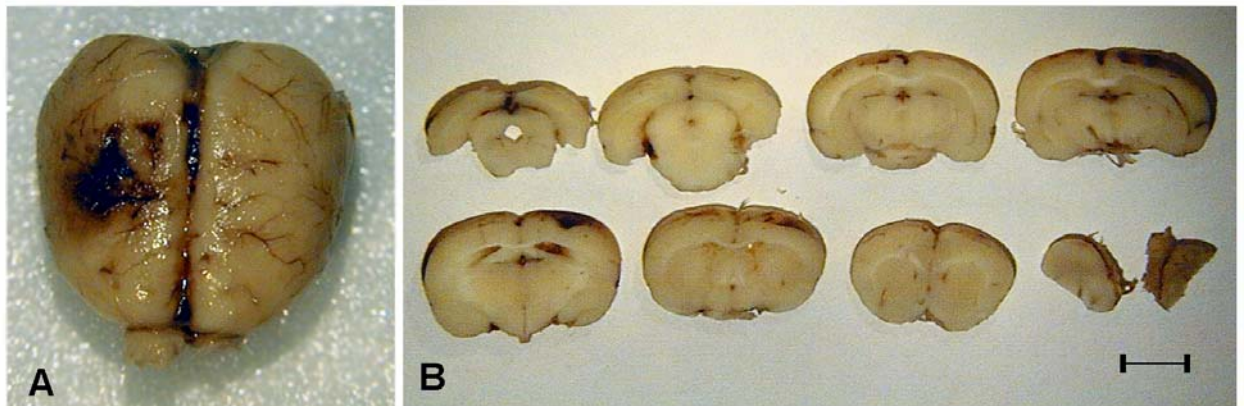


**Figure 14:** Brain of an animal after photothrombotic stroke formation. The whole brain is seen in panel A where a lesion can be seen on the cortical surface. B shows slices through this brain. Bar equals 1cm.

#### **4.4.5 Macrosphere and Suture MCAO Model**

With conventional ischemic imaging studies being carried out in anesthetized animals for the duration of the imaging session, it was hypothesized that this anesthesia might have an effect on the outcome of the stroke. An experiment was designed to compare these two treatments to each other and to a more conventional method of stroke induction; anesthetized suture MCAO. The most important factor in the design of this experiment was the absence of anesthesia in the awake group from the time of stroke induction until the end of the experimental period. The other cohorts remained anesthetized for a period that corresponded to an average MRI experiment (90 minutes).

The two macrosphere groups received spheres via an arterial catheter, one group while the animal was anesthetized, and the other while the animal was awake. Anesthesia was continued in the first cohort and the suture MCAO group, and physiologic monitoring was continued in all three groups for the first 90 minutes after induction. After this time all of the animals were returned to their home cage and allowed to recover. Twenty four hours later all animals were sacrificed and fixed for post mortem examination.

These experiments were feasible in awake animals, and showed histological differences between awake and anesthetized groups. Several important differences were noted in the physiology of these animals during the time of the stroke that might account for a pathological difference. There were also many similarities between the anesthetized macrosphere group, and the suture stroke group showing a similarity

The study was successful in awake animals. Of the awake animals in the study, 7/11 (64%) had spheres enter the cerebral circulation, but one was unusable histopathologically. In the anesthetized group, 7/10 (70%) had spheres enter the cerebral arteries. For comparison, the suture MCAO model is a very consistent method and all of the trials were successful despite some respiratory problems from the anesthesia. It should be noted, however, that the suture model was done only in anesthetized animals. (Table 2)

Some of the animals died during the stroke induction and were excluded from the study, but are noted for methodological reasons. All of these animals (n=6) expired after pulling out arterial catheters during struggling. Death occurred after injection of microspheres and 50% of these animals had spheres lodged in their cerebral arteries. (Table 2). All but one of these animals were from the same litter which seemed to have markedly weaker arteries and all had complications during the study.

	Sacrificed in 24 hours .						Died during restraint.		
	Total	# with MCA occlusion	Without	Died over night	Resp problems	scored zero despite spheres	Total	With spheres	Without
Awake	11	7	4	1	0	0	6	3	3
Sedated	10	7	3	1	3	1	0	0	0
Suture	8	8	0	0	2	0	0	0	0

**Table 2:** The success rate of macrosphere induced stroke in study subjects. Numbers are also given for the suture MCAO model for comparison.

Complications also occurred during the preparation of both the anesthetized and suture groups attributed to respiration failure from prolonged

inhaled anesthesia. 30% in the sedated group and 25% of the suture group had respiratory problems of varying degrees. (Table 2)

The distribution of the spheres seemed consistent between the two cohorts with most of the spheres entering the distal ICA and the MCA (Table 3) which were the intended target for the spheres. Interestingly, the mean number of spheres that entered into the brains is different ( $p=.002$ ) between the two groups.

Cerebral Artery	Awake	Anesthetized
Internal Carotid	6	6
Middle Cerebral	5	6
Anterior Cerebral	1	3
Posterior Comm.	1	3

**Table 3:** Location of spheres in the cerebral arteries.

The anesthetized group had more spheres found post mortem (mean= 5.4) compared to the awake group (mean= 3.2). This is probably attributed to the direct visualization of the spheres in the anesthetized group as they were injected into the proximal portion of the ICA. This might also account for the higher success rate in the anesthetized cohort. Figures 15 and 16 show all of the brains used in the study for the anesthetized and awake cohorts respectively. The red arrows indicate the locations of the spheres.

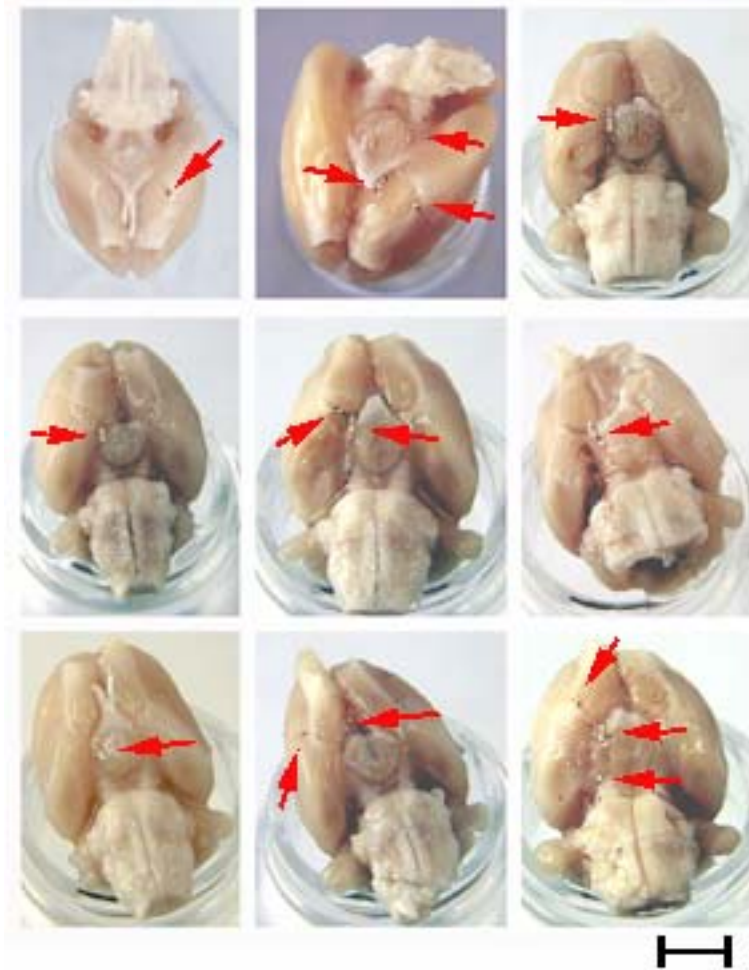


**Figure 15:** Location of macrospheres in the cerebral arteries of the sedated group. Photographs of each of the 9 brains in the study that contained macrospheres from anesthetized animals. When compared to figure 16 it is noted that this cohort had a higher number of spheres in the brain. Red arrows indicate sphere locations. Bar equals 1cm.

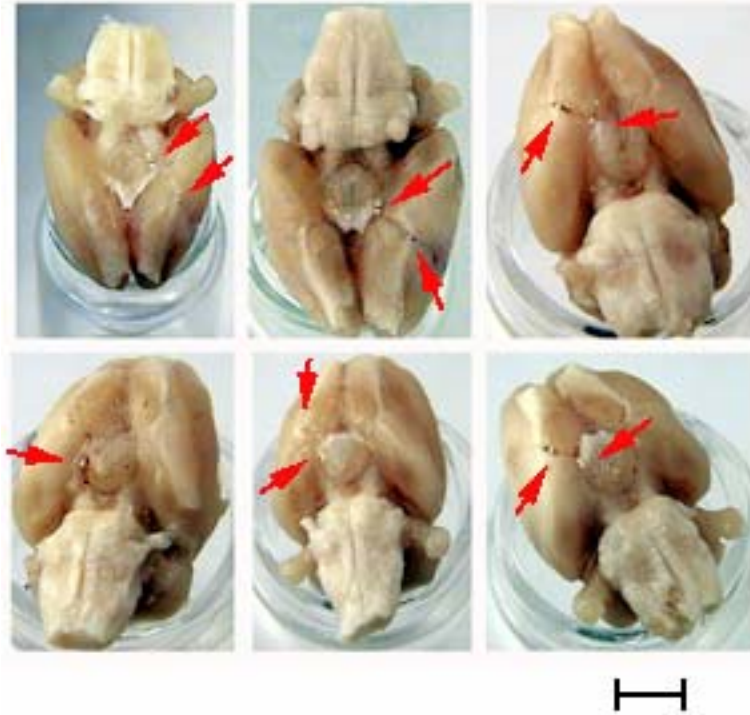


**Figure 16:** Location of macrospheres in the cerebral arteries of the awake group. Photographs of brains from the 6 awake animals in the study. Red arrows indicate sphere locations. Bar equals 1cm.

The suture MCAO model is a very straightforward model and produced no complications. Figure 17 shows the remnants of the suture (arrow) lodged in the distal ICA. All of the brains had suture lodged in the distal MCA upon post mortem inspection. Figure 17 shows an example brain with the suture seated in the distal ICA, effectively blocking the MCA.

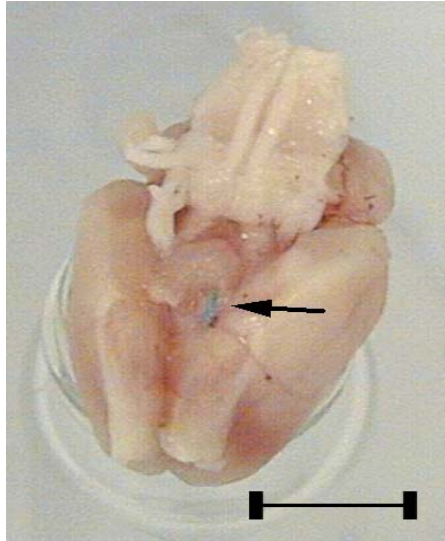


**Figure 17:** Suture MCAO brain showing the suture lodged into the anterior cerebral artery. The arrow indicates the remnants of the artery. The remainder of the suture was cut away when the brain was extracted. Bar equals 1cm.

All animals maintained fair health after the stroke. The blood gas and pH was consistent between the two macrosphere groups and before and after time points for each group. Table 4 shows the values for  $PO_2$ ,  $PCO_2$ , and pH for each cohort at time points before and after the injection of the macrospheres. Other studies on awake animals (Nakao, 2001) have noted that the primary physiologic difference between the awake and anesthetized group was a higher  $PaO_2$  and pH in the anesthetized group. Differences in these studies, and in ours (not statistically significant), might be attributed to the anesthetized group receiving the isoflurane in pure oxygen while the awake animals inhale room air.

	Awake Before	After	Sedated Before	After	Suture Before	After
PO2	92.3 (12.1)	104 (32.5)	94.0 (5.0)	87.5 (4.2)	106 (7.8)	97.8 (7.1)
PCO2	34.9 (4.7)	32.7 (1.3)	32.5 (3.8)	37.0 (5.5)	31.4 (4.7)	33.7 (6.9)
PH	7.44 (.04)	7.43 (.04)	7.45 (.02)	7.44 (.02)	7.47 (.06)	7.47 (.03)
Glucose	133 (34.5)	102 (27.3)	114 (18.3)	93.5 (11.1)	139 (20.5)	99.2 (11.5)

**Table 4:** Blood gas and metabolite concentrations in animals pre and post stroke. No

statistical difference was found between the before and after measurement (paired t test), nor among the cohorts (Kruskal Wallis/ Dunns test). Values expressed as mean(sd).

### *Stroke Outcome*

The awake group had a markedly increased lesion compared to the anesthetized and suture groups (Table 5;  $p < .01$ ). The lesion volume in the anesthetized group was comparable to the volume of the anesthetized suture group. There was no significant difference in the neurological scores of the groups, however. This model showed virtually identical edema, quantified by % hemisphere volume among the groups. The percent hemispheric volume of the right hemisphere in table 5 indicates this.

	Awake	Sedated	Suture
% Hemisphere Lesion Volume	31.3 (14.6)**	15.8 (6.1)	11.4 (6.4)
Lesion Volume (mm <sup>3</sup> )	119.9 (67.4)**	51.8 (31.2)	38.5 (21.9)
# of spheres	3.2 (0.8)**	5.4 (0.5)	
% Hemisphere Volume	53.4 (2.9)	53.7 (3.1)	52.2 (1.3)
Neuro score	1.3 (0.5)	2.3 (1.2)*	1.9 (0.4)
Temperature	38.4 (0.4)	37.6 (1.1)	38.9 (.3)*

**Table 5:** Outcome of the macrosphere and suture subjects 24 hours after stroke.

Statistical difference as noted (\*  $p < .05$ , and \*\*  $p < .01$ ; Kruskal Wallis/ Dunns test).

Values expressed as mean(sd).

Both hematoxylin and eosin (H and E), and thionin stains can delineate a lesion after 24 hours. Figure 18 shows examples of each stain for the same lesioned brain. It also shows the differences at a higher magnification.

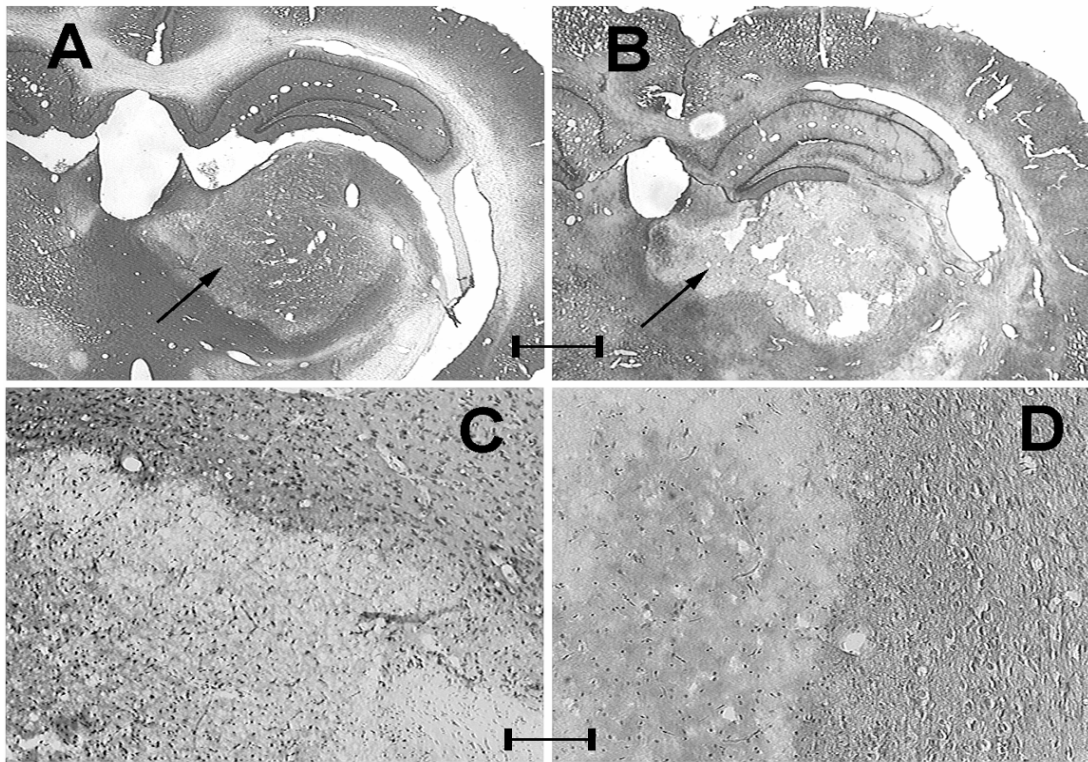


**Figure 18:** Histology of ischemic lesions. A shows a lesion stained with thionin while B shows the same lesion in a hematoxylin and Eosin stained section. The lesion is easily distinguished (arrows) in both stains as a light area with no noticeable nuclei. C and D show higher magnification (100x) of the lesion boundaries. At this higher magnification it is possible to see the shrunken and much less abundant nuclei in the ischemic zone (area not containing the letters). C is the thionin stain while D is the H and E stain. Bars in A and B equal 1mm. Bars in C and D equals 100µm.

The physiology of the awake and anesthetized cohorts differed greatly from each other. Along with the differences between groups, changes in the physiology from the point after the stroke induction were notable. Of these post stroke changes, the largest and most variable were in the anesthetized group. Table 6 shows several physiologic variables initially, and after the stroke for the awake, anesthetized and suture cohorts.

	Awake Before	After	Sedated Before	After	Suture Before	After
MABP	139.5 (14.6)**	146.2 (12.7)	105 (11.7)	105.3 (10.5)	110.3 (14.3)	100 (15.5)
Heart Rate	398 (41)**	424 (45.7) $\tau$	306 (44.9)	362 (17.1) $\tau$	332 (16.7)	316 (61.2)
Temperature	36.5 (.8)	37.3 (.5)	37.1 (.8)	37.7 (1.5)	37.2 (0.7)	37.4 (0.3)
SpO <sub>2</sub>	74.7 (7.8)**	88.5 (5.0) $\tau$	94.5 (2.6)	92 (3.3)	89.1 (5.0)	92.2 (2.3)

**Table 6:** Physiologic measures of the awake, anesthetized, and suture MCAO groups.

Statistical difference was found between the before and after measurement ( $\tau$   $p < .05$ ; paired t test), and among the cohorts before measurements as noted (\*  $p < .05$ , and \*\*  $p < .01$ ; Kruskal Wallis/ Dunns test). Values expressed as mean(sd).

Differences among the cohorts were noted in BP, HR, and SpO<sub>2</sub> as seen in table 6. The awake cohort had a higher BP and HR than the anesthetized groups. The awake group also had a lower SpO<sub>2</sub> than the anesthetized groups, probably because of the anesthesia being delivered in oxygen to the sedated groups.

The awake group also had the greatest differences in physiology before and after the induction of the stroke. The heart rate increased significantly in both the anesthetized and awake groups. The BP was constant in the awake, anesthetized, and suture groups before and after stroke. The SpO<sub>2</sub> and PO<sub>2</sub> of the conscious group increased after the macrosphere injection but stayed

constant in the other groups. The increase might be attributed to the awake animals recovering from isoflurane anesthesia during this period and their respiration clearing up after inhaling the dry gas for the entire surgical procedure. Figure 19 shows sample traces of the physiology measures of each of the cohorts and one awake control animal for a period before, and 90 minutes after the stroke induction.

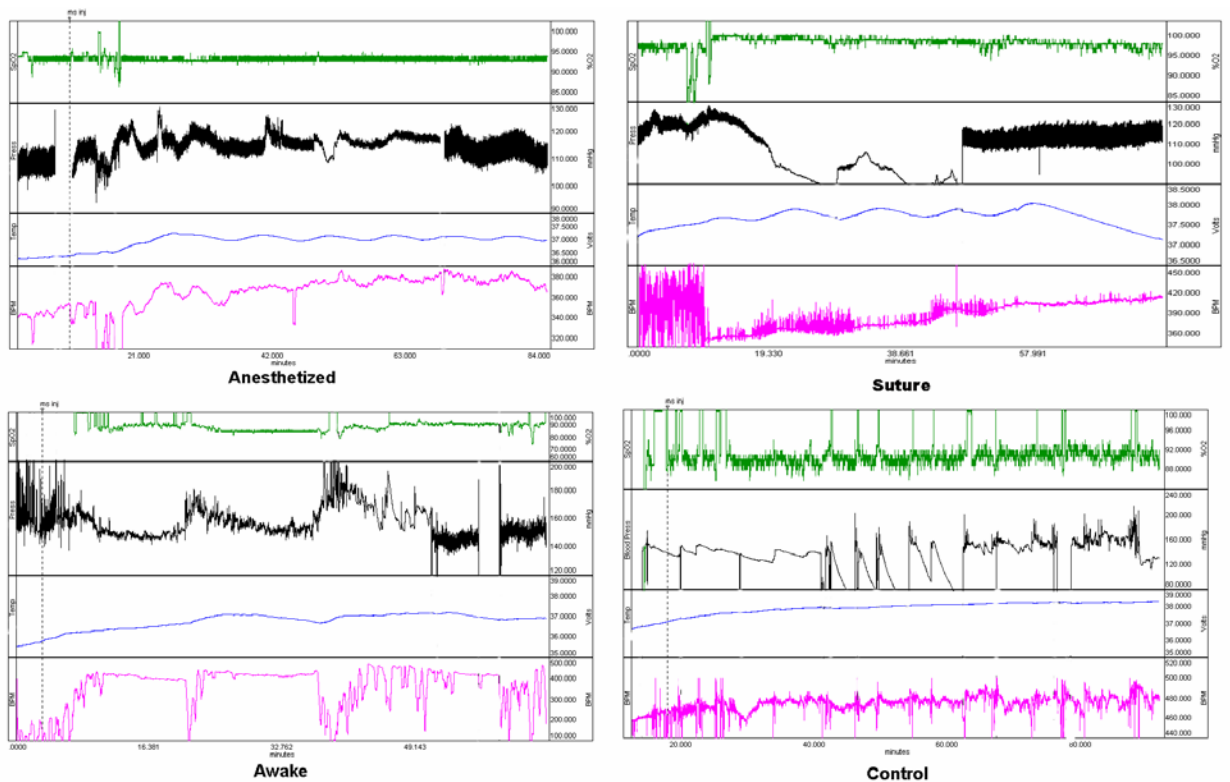


**Figure 19:** Physiologic profile of a macrosphere and suture MCAO Model in an anesthetized, awake, and awake control animal. The vertical dotted lines indicates the point of sphere injection. The top trace is of an anesthetized animal, the middle an awake animal, and the lower is in an awake animal that received a sham injection. Gaps in the BP signal were caused by loss of patency of the catheter. The signal loss in the BP channel of the suture animal resulted from lost patency of the catheter. The problem was cleared and the signal returned to normal.

## 5. Discussion

**N**ew equipment and methods were successfully brought together for conducting stroke studies with conscious animals. The equipment provided a broad range of physiologic data in both invasive and non invasive manners. Anesthesia was utilized when necessary for animal preparation, but was then eliminated during the actual study. The effects of stress on the subject animal were studied and conditioning was shown to limit these effects. Several models were feasible for the two major forms of stroke, occlusive and hemorrhagic, that work on awake animals within the MRI apparatus. Lastly, experiments using a macrosphere model showed evidence of a pathophysiologic difference between awake and anesthetized animals that undergo stroke.

### ***5.1 Physiology System***

The system that was created for physiologic data acquisition was designed with several criteria in mind. First, all the sensors that were placed within the magnet had to be MRI compatible. This meant that there could be no ferromagnetic materials used in their construction. It was also important that the data be coordinated, displayed, and stored digitally. This ensured temporal consistency between all of the parameters and the imaging equipment, as well as easier handling of data.

All of the physiologic equipment functioned well, but performance varied depending on the experiment. The EKG was best for calculating the heart rate,

but the tail pulse sensor also worked well for non invasive HR provided the animal had good circulation. The pulse oximeter worked better when it was placed on a limb, but an awake animal often kicked it loose. Tail placement worked also, but the signal was never as accurate as when a limb was used.

Measuring a direct blood pressure avoided the shortcomings of the NIBP monitor when the animal was under stress. Because of the extensive surgery that direct BP monitoring requires, however, it is only necessary if blood needs to be sampled or if very accurate and constant BP is necessary. For instance, in the SPSHR study the BP increase could not be measured with the NIBP equipment because of altered peripheral circulation so a direct catheter was used.

The intrathecal catheter provided an accurate ICP measurement. The primary drawback to this method is the sensitivity to the position of the pressure transducer. In order to achieve accurate measurements, it was important to keep the transducer level with the spine at all times.

## ***5.2 Anesthesia***

Domitor was successful as a fully reversible anesthetic. Full surgical procedures were possible under a more consistent sedation than isoflurane provided, and respiratory side effects were not encountered. Reversal was quick and complete with physiology and EEG returning to conscious levels within 2-4 minutes. There are many studies on the effects of isoflurane on CMR, CBF, and other factors that can affect stroke outcome, but none of these factors has been studied with medetomidine anesthesia. The information available on isoflurane allowed for a better analysis of how it affected stroke outcome in the

macrosphere model based on previous studies. The use of mild isoflurane anesthesia at the end of the restraining sessions proved very advantageous to limit the complications experienced while removing the animal from the restrainer. This technique was only implemented in a few studies, however (the ICH and SAH models).

### ***5.3 Stress Studies***

The stress studies indicated that experimental animals should be given 5 sessions of habituation to the restrainer before experimentation. This protocol would limit stress in the animals as it may affect the outcome of the stroke. Procedurally, habituation should reduce the extemporaneous movements of the animal in order to limit complications that come from struggling such as pulled catheters. During the SPSHR study, stress was thought to aid in increasing the animals BP and possibly precipitating stroke.

### ***5.4 Stroke models***

Stroke studies are hindered by the current experimental designs in stroke modeling. Besides the poor temporal resolution of some methods, the lack of an adequate awake control condition calls into question conclusions drawn from anesthetized studies. As an example, Warner et al (1991) used autoradiography to track CBF changes in MCAO models and evaluate cerebral perfusion and outcome. They found that different anesthetics have different thresholds for tissue damage because they have varying effects on CMR and CBF.

Unfortunately, there has never been a thorough time course study of these factors in an awake animal with which to compare the data.

Awake stroke models presented a number of methodological complications. Mechanical stroke induction often required an immobilized animal. While some previous models incorporate awake, freely moving animals (Demura, 1993) most studies utilize anesthesia to stabilize the animal in order to access the arteries. Awake models require that all surgeries are closed and any externalized lines secured. This adds complications to the procedures and makes the long term survival of the animal more difficult when they are disconnected from experimental equipment such as catheters.

The macrosphere model exemplified most of these concerns. Compared to the anesthetized suture MCAO model, the awake model was more difficult to use and less successful. While the suture MCAO was a simpler model, it was still prone to complications from anesthesia. When the macrosphere model was used with anesthetized animals, it was almost as consistent and simple to prepare. The awake method for macrosphere MCAO is a feasible model as it allows the experimenter to rule out many variables that anesthesia introduces.

A difference was noted between awake and anesthetized animals in the macrosphere model. Anesthetized animals had a decrease in lesion volume and a higher MABP and these differences have been seen in other studies that have compared gas anesthetized animals to awakening animals. Kawaguchi et al (2000) found a 50% reduction in the lesion size of isoflurane anesthetized animals (43 mm<sup>3</sup> anesthetized, 86 mm<sup>3</sup> awake) when lesion size was evaluated

with H&E staining. Warner et al (1995) saw a 46% reduction in lesion size in halothane anesthetized animals (106 mm<sup>3</sup> anesthetized, 197 mm<sup>3</sup> awake). There are several differences in the awake and anesthetized animal models that could account for pathological differences including lower CBF, CPP, and CMR in the anesthetized group, and lower physiologic oxygen and increased catecholamines (from stress) in the awake animals could account for differences. The difference in stroke outcome between an awake and an anesthetized model is a large one. Since an awake model is a better replication of the human condition during stroke, it might be worth the added complications of setting up awake studies.

A decrease in cerebral blood flow has been found to coincide with a decrease in infarct volume since the perfusion pressure, which is related to CBF, can affect the at-risk area and the actual area of infarction (Warner 1991). The MABP of the awake and anesthetized group were significantly different from each other, and might be responsible for the difference in lesion volume.

The reduction of CMR caused by anesthesia can result in neuroprotection. The hypothesis for neuroprotection from CMR reduction is that the decreased metabolic rate corresponds with a decreased delivery of fuel to the compromised area. Isoflurane allows a higher cerebral blood flow while reducing cerebral metabolism, and studies show that isoflurane can reduce the cerebral metabolic rate (CMR) by 42% when compared to halothane. This corresponds with a decrease in ischemic damage (Nellgard, 2000).

The peripheral metabolism showed little difference between the awake and sedated cohorts. The blood gasses and pH stayed fairly constant while the glucose levels decreased slightly after the injection of the macrospheres.

Hyperthermia can have a detrimental effect on neurologic outcome and often accompanies many stroke models. It is proposed that anesthetics provide neuroprotection by suppressing hyperthermia. After CBF, temperature appears to be the second most important factor for stroke severity (Jacewicz, 1986) More consistent cortical temperatures in anesthetized animals may have more to do with outcome than the metabolic and vascular effects of anesthesia. Warner et al (1995) found a 46% reduction in infarct size in animals that were anesthetized with halothane during ischemia and reperfusion so long as the animals' cranial temperature was controlled and remained normothermic.

Catecholamines are important substances in cerebral mechanics, and can be suppressed by anesthesia. Theoretically, catecholamines can directly affect many of the other proposed causes of neuroprotection, but the role that these compounds have in the progression of stroke is very unclear.

While stroke induction in the SPSHR model can be done in a noninvasive manner (Brevard, 1999), invasive preparations were required to monitor the animal. This gave the experiment one chance for success, since the animal had to be sacrificed afterwards. Timing of the experimental intervention in order to induce stroke was crucial. Many criteria determine this readiness to stroke, and it is difficult to pinpoint animals in this state. Still, this model is feasible. Non

invasive methods for induction that can be repeated in the same animal might prove to be more efficient.

Both the SAH and ICH models work well within the restraining apparatus. The SAH model is a bit harder to perform, but is still a feasible model. These models might serve as good controls to the spontaneous hemorrhage model. The suture MCAO served as a good control for the anesthetized macrosphere cohort. The photothrombotic model was unsuitable for our experiments.

## **5.6 Histology**

Assessment of lesion volume varies with histological methods. Tetrazolium salts offer a good marker for ischemic lesion volume; however, it is an exclusive staining method that eliminates the possibility of using other stains. For that reason Hematoxylin and Eosin (H and E) staining was chosen for the macrosphere studies in order to leave other staining options open. H and E was highly variant and nissl stains were used in conjunction to define lesion boundaries.

Warner et al (1995) found that H and E staining gave lesion volumes that were 11% greater than with tetrazolium staining. Our lesion volumes were much lower than those previously published for the suture MCAO and anesthetized macrosphere model (Garriets, In Print), but these studies used tetrazolium staining to assess lesion volume and also used chloral hydrate for anesthesia. In pilot studies in our lab we find lesion volumes in isoflurane anesthetized animals are markedly smaller than those in animals anesthetized with chloral hydrate (not

published). In this study our findings are more comparable to Kawaguchi et al (2000) who used H&E staining to assess a suture reperfusion model.

A combination of these methods where alternate 1mm thick slices are stained with tetrazolium salts and the other section is fixed for slicing and staining via other methods might be advisable. This should allow for accurate volume assessment along with more eloquent markers for cellular integrity.

When scanning the lesion volumes, the brain of one anesthetized rat posed the baffling situation that it had no apparent lesion on any of the slices. When going over the rest of the records for this animal, it was discovered that this rat had scored a zero on its neurological evaluation despite the postmortem detection of spheres. In other animals, the neural score seemed to have little to do with the histopathologic outcome of the stroke. If one were to investigate the relationship between neural score and stroke pathology, a larger number of trials would have to be used in order to statistically illustrate this discrepancy.

## ***5.6 MRI as a tool to investigate stroke***

The acuity of MRI might help us to better quantify stroke severity in the models. Stroke severity can be gauged by the change in neurological function, gross pathology, cellular morphology, or any combination of the three. Current dogma with stroke models is to base outcome almost entirely on the two factors of simple neurological scores and infarct volume measurements. Clinical assessment of stroke has largely to do with a more complex look at neurological function which has little correlation to infarct volume (Aronowski, 1996). Molinari (1986) commented that researchers should strive for consistency in evaluation

between models and the clinical setting. Since it is function that clinicians are most worried about restoring and maintaining in the clinical population, neurological scoring is a common clinical determinate of stroke severity. While neurological scoring is used in animal models, the criteria for humans are more complex. The size of an infarction is irrelevant if function has been redistributed to other locations in the brain. This phenomenon has been demonstrated in fMRI evaluation of clinical lesions (Thulborn, 2001). If both of these measures can be ambiguous in their implications on stroke severity then neurological scores and infarct volume seem inadequate to establish stroke severity in models. Studies have noted a poor correlation between these two variables (Warner, 1991).

Stroke severity can be assessed in terms of functional changes during and after a stroke. Some of these changes can be detected using functional MRI. These functional losses can be the result of specific injury to neurons that cannot be detected by conventional MRI sequences or even conventional histological staining (Patel et al, 1999).

Conventional methods for tracking CBF have also posed limits on previous stroke studies. LDF and other minimally invasive CBF measurement techniques are limited to the cortical areas for recording. Warner et al (1991) used autoradiography to track CBF changes in MCAO models throughout the brain. They concluded that this method provided adequate resolution to discern differences in intraschemic blood flow. However, these methods are temporally limited to one time point since they require the sacrifice of the animal. MRI

sequences sensitive to CBF would be accurate at tracking changes in perfusion over a broad time course.

We are able to study the oxygen consumption using BOLD based imaging modalities and can potentially do a more thorough study of CMR as it relates to ischemia. In vivo spectroscopy could offer a glimpse at glucose consumption and waste product accumulation. These methods might help us image intracerebral steal.

Another important study would be to assess brain function and viability as it relates to brain and core temperature. Such a study might give a better sense of how temperature relates to stroke outcome. An MRI study might also reveal a time course to the progression of ischemic damage as it relates to temperature.

## ***5.7 Conclusions***

Stroke is the major neurological problem facing our healthcare system today. While extensive time and resources have been dedicated to preventing and treating strokes, no major treatment scheme, pharmacologic or physiologic, has proven itself capable of handling our stroke patient population. A major clinician and researcher in the field of stroke, Marc Fisher, cites the lack of translation of new neuroprotective drugs into viable human drugs. These compounds help reduce the impact of stroke when tested with animal models, however, when they then applied to the patient population, each of these drugs failed to reduce the damage of stroke. One cause of this discrepancy between stroke models and stroke patients could be in the unrealistic pharmacologic and physiologic condition of current animal models when compared to

unanesthetized humans. It would stand to reason that a more realistic stroke model would utilize awake animals. This work marks a new direction in the exploration of stroke in animal models that might, some day, help us better manage cerebrovascular trauma.

## 6. References

Bederson JB, Germano IM, Guarino L. Cortical blood flow and cerebral perfusion pressure in a new noncraniotomy model of subarachnoid hemorrhage in the rat. *Stroke* 1995 ;26,6: 1086-1091.

Benveniste H, Kim KR, Hedlund LW, Kim JW, Friedman AH. Cerebral hemorrhage and edema following brain biopsy in rats: significance of mean arterial blood pressure. *Journal of Neurosurgery* 2000; 92: 100-107.

Brevard ME. Magnetic resonance imaging of hemorrhagic stroke in conscious rats. 1999. Major Qualifying Project for Worcester Polytechnic Institute.

Brinker T, Siefert V, Dietz H. Cerebral blood flow and intracranial pressure during experimental subarachnoid haemorrhage. *Acta Neurochirurgica* 1992; 115: 47-52.

Coutard M, Huang W, Osborne-Pellegrin M. Heritability of intracerebral hemorrhagic lesions and cerebral aneurysms in the rat. *Stroke* 2000;31: 2678-2684.

Coyle P, Feng X. Risk Area and Infarct Area Relations in the Hypertensive Stroke-Prone Rat. *Stroke* 1993; 24,5: 705-709.

Gerriets T, Li F, Silva MD, Meng X, Brevard ME, Sotak CH, Fisher M. The Macrosphere Model- Evaluation of a New Stroke Model for Permanent Middle Cerebral Artery Occlusion in Rats. Accepted to J. Neurosci. Methods. 2002

Heistad DD, Kontos HA, Cerebral Circulation, in Shepherd JT, Abboud FM, Gieger SR. Handbook of Physiology Section 2 The cardiovascular system Vol 3. 1983 The American Physiology Society.

Jacewicz M, Pulsinelli WA. Animal Models of ischemia. in Barnett HMJ, Mohr JP, Stein BM, Yatsu FM Stroke Pathophysiology, diagnosis and management. 1986 Churchill Livingston Inc,

Jamali S, Bodjarian N, Bernard V, Mazoit J, Samii K, Tadie M. Increase in the chronically monitored cerebrospinal fluid pressure after experimental brain injury in rats. *Brain Injury* 1998; 12,6: 525-536.

Kawaguchi M, Kimbro JR, Drummond JC, Cole DJ, Kelly PJ, Patel PM. Isoflurane Delays but Does Not Prevent Cerebral Infarction in Rats Subjected to Focal Ischemia. *Anesthesiology* 2000; 92; 1335-42.

Lahti KM, Ferris CF, Li F, Sotak CH, King JA. Imaging brain activity in conscious animals using functional MRI. *J Neurosci Methods* 1998;82:75-82.

Lahti KM, Ferris CF, Li F, Sotak CH, King JA. Comparison of evoked cortical activity in conscious and propofol-anesthetized rats using functional MRI. *Magn Reson Med.* 1999;41:412-216.

Longa EZ, Weinstein PR, Carlson S, Cummins R. Reversible middle cerebral artery occlusion without craniectomy in rats. *Stroke* 1989; 20: 84-91.

Molinari GF. Experimental models of ischemic stroke, in Barnett HMJ, Mohr JP, Stein BM, Yatsu FM Stroke Pathophysiology, diagnosis and management. 1986 Churchill Livingstone Inc,

Nakao Y, Itoh Y, Kuang T, Cook M, Jehle J, Sokoloff L. Effects of anesthesia on functional activation of cerebral blood flow and metabolism. *PNAS* 2001;98,13: 7593-7598.

Nath FP, Kelly PT, Jenkins A, Mendelow AD, Graham DI, Teasdale GM. Effects of experimental intracerebral hemorrhage on blood flow, capillary permeability, and histo chemistry. *Journal of Neurosurgery* 1987; 66: 555-562.

Nellgrad B, Mackensen B, Massey G, Pearlstein R, Warner DS. The Effects of Anesthetics on Stress Responses to forebrain Ischemia and reperfusion in the Rat. *Anesth Analg* 2000;91: 145-151.

Osborne PG, Denton DA, Weisinger RS. Cerebrospinal fluid pressure of anaesthetized rats during intracerebroventricular infusion. *Physio Behav* 1986;37:1-4.

Patel TR, Schielke GP, Hoff JT, Keep RF, Betz AL. Comparison of cerebral blood flow and injury following intracerebral and subdural hematoma in the rat. *Brain Research* 1999 ;829: 125-133.

Ridenour TR, Warner DS, Todd MM, Gionet TX. Comparative Effects of Propofol and Halothane on Outcome from Temporary Middle Cerebral Artery Occlusion in the Rat. *Anesthesiology* 1992; 76: 807-812.

Sankar R, Shin DN, Wasterlain CG. Serum Neuron-specific enolase is a Marker for Neuronal Damage Following Status Elipticus in the Rat. *Epilepsy Research* 1997; 28: 129-136.

Schwartz A, Masago A, Sehba F, Bederson J. Experimental models of subarachnoid hemorrhage in the rat: a refinement of the endovascular filament model. *J Neurosci Methods* 2000;96:161-167.

Smead JS. Hemorrhagic Stroke Development in spontaneously hypertensive rats fed a north american, japanese-style diet. *Stroke* 1989; 20: 1212-1218.

Thulborn KR. Clinical applications of fMRI: Bold claim or reality? Plenary Lecture at 9<sup>th</sup> annual meeting of the International Society for Magnetic Resonance in Medicine. April 2001, Glasgow, Scotland, UK.

Tintinall JE, Kelen GD, Stapczynsk JS. Emergency Medicine: A Comprehensive Study Guide 5<sup>th</sup> Edition. © 2000 Mcgraw Hill.

Veelken JA, Laing RJC, Jakubowski J. The Sheffield Model of Subarachnoid Hemorrhage in Rats. *Stroke* 1995; 26,7:1279-1283.

Watson BD, Dietrich WD, Watchel M, Ginsberg MD. Induction of reproducible brain infarction by photochemically initiated thrombosis. *Ann Neurology* 1985; 17: 497.

Warner DS, Zhou J, Ramani R, Todd MM. Reversible Focal Ischemia in the Rat: Effects of Halothane, Isoflurane, and Methohexital Anesthesia. *Journal of Cerebral Blood Flow and Metabolism* 1991; 11: 794-802.

Warner DS, Ludwig PS, Pearlstein R, Brinkous AD. Halothane Reduces Focal Ischemic Injury in the Rat When Brain Temperature is Controlled. *Anesthesiology* 1995; 82: 1237-1245.

Warner DS, Takaoka S, Wu B, Ludwig PS, Pearlstein RD, Brinkous AD, Dexter F. Electroencephalographic burst suppression is not required to elicit maximal neuroprotection from pentobarbital in a rat model of focal cerebral ischemia. *Anesthesiology* 1996; 84: 1475-1484.

Wiebers DO, Adams HP, Whisnant JP. Animal models of stroke: Are they relevant to human disease? *Stroke* 1990; 21,1: 1-3.

## 7. List of Abbreviations

ACA- anterior cerebral artery  
BBB- blood brain barrier  
BOLD- Blood Oxygen Level Dependant  
CBF- cerebral blood flow  
CCA- common carotid artery  
CMR- Cerebral Metabolic Rate  
CPP- cerebral perfusion pressure  
CSFP- Cerebrospinal fluid pressure (equivalent to ICP)  
ECA- external carotid artery  
EEG- Electroencephalograph  
EKG- Electrocardiograph  
ICA- Internal carotid artery  
ICH- Intracerebral hemorrhage  
ICP- intracranial pressure  
LDF- Laser Doppler flow  
MABP - mean arterial blood pressure  
MCA- middle cerebral artery  
MCAO- medial cerebral artery occlusion  
MRI- Magnetic resonance imaging  
SAH- Subarachnoid hemorrhage  
SNN- specific neuronal necrosis  
PCA- posterior cerebral artery